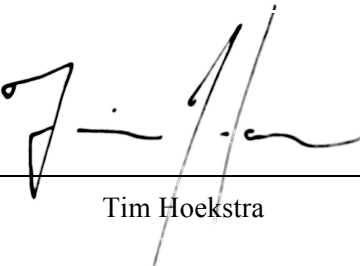




NON-DESTRUCTIVE TESTING OF CARBON FIBER CRANK ARMS

Final Design Report

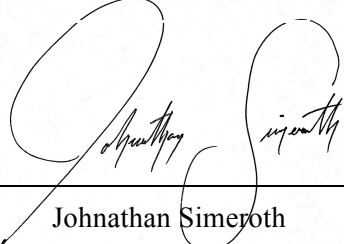
December 8, 2016



Tim Hoekstra



Grant Pocklington



Johnathan Simeroth

Sponsors:
SRAM
Dr. John C. Chen

Mechanical Engineering Department
California Polytechnic State University
San Luis Obispo

Table of Contents

List of Figures	3
List of Tables	4
Abstract.....	5
I: Introduction.....	5
Team Management Plan.....	6
II: Background.....	7
Carbon Fiber Reinforced Polymer (CFRP).....	7
Vibrothermography and Dr. John C. Chen’s Procedure and Setup.....	10
Visual Inspection.....	13
Laser Ultrasonic Testing.....	13
Thermal Pulse Thermography.....	13
Lock in Thermography.....	14
LED Optical Excitation.....	14
X-Ray Testing.....	14
III: Design Development.....	15
Requirements / Specifications.....	15
Concept Generation.....	16
Idea Selection.....	16
IV: Description of the Final Design.....	18
Design Development History.....	18
Final Design.....	21
V: Testing Information.....	22
Test Plan.....	22
Control Testing.....	23
Optimized Test Parameters.....	23
VI: Results and Analysis.....	24
Image Analysis.....	24
Results.....	28
VII: Conclusion.....	30
VIII: Topics for Additional Research.....	31
Originally Proposed Fixture.....	31
True NDT and Automation.....	31
Sine Sweep Thermography.....	31

Appendices.....	33
A - Gantt Chart.....	34
B - Quality Functional Design.....	35
C - Design Goals Concept Selection Matrix.....	36
D - Cost Report.....	37
E - Test Plan.....	38
F - Manufacturing Plan.....	42
G - DFMEA.....	44
H - Drawing Package.....	45
I - Summary of Testing Inputs and Outputs.....	63
References.....	64

List of Figures

Figure 1	Laminates damage from impact testing	6
Figure 2	Crank arm cutaway	7
Figure 3	Bicycle with crank arm location	8
Figure 4	SRAM Force crank arm	8
Figure 5	Isotropic vs. anisotropic materials	9
Figure 6	Carbon fiber weaves	9
Figure 7	Testing setup side view	10
Figure 8	Testing setup clamps	11
Figure 9	Test coupon example static	12
Figure 10	Test coupon example as seen during testing	13
Figure 11	Fixture concept 1 utilizing back plates	18
Figure 12	Upright front view	19
Figure 13	Spindle mount plate	20
Figure 14	FEA frequency analysis at 28th natural frequency	20
Figure 15	Final cantilever fixture	21
Figure 16	Final cantilever fixture set up on existing uprights	22
Figure 17	Steel pedal nub used to avoid surface damage	24
Figure 18	Raw image from testing	25
Figure 19	Testing image with increased contrast; pre-excitation image	26
Figure 20	Testing image with color mapping	26
Figure 21	Pixel image subtracted from all cells of testing images	27
Figure 22	Fatigued crank arm with pixel image subtracted from all cells during testing	28
Figure 23	Cantilever test image showing disbond area around pedal lug	29
Figure 24	Cantilever test image of disbond area around pedal lug using different gun location	29
Figure 25	Indication of a testing-induced defect	30
Figure 26	Pedal nub absorbing all the energy on fatigued and non-fatigued crank arms	30

List of Tables

Table 1 Fixture design goals

17

Abstract

Carbon fiber components present unique challenges for detecting defects, damage, and fatigue. Nondestructive methods exist for testing and locating defects. However, most of these methods are expensive, not versatile enough for practical use on non-idealized parts, or both. Vibrothermography can be an affordable option and has shown promising results with thin rectangular panels. The goal of this senior project was to assess the feasibility of using vibrothermography to find defects in SRAM carbon fiber crank arms. Our team found vibrothermography to be a feasible method of non-destructive testing for carbon fiber crank arms, and this report discusses the development and implementation of the necessary theory, fixturing, and testing procedures.

I: Introduction

Carbon Fiber Reinforced Polymer (CFRP) is a composite material that is composed of layers of carbon fibers that are saturated and held together with a cured epoxy. Unlike most materials, carbon fiber tends to develop defects below the surface, making defects difficult to detect. A type of defect specific to a layered composite like CFRP is a delamination, or separation, of two of the fiber layers from one another in an area. This can occur from impurities in the work environment during manufacturing or from impact or fatigue while in use. Figure 1 shows cross-sectional views of delaminations in several impact test specimens. In three of the four test specimen shown, the surface where the impact occurred--the top layer--is not visibly broken. However, layers beneath the surface are fractured. For small surface dents, sometimes these defects can be undetectable. In order to find internal delaminations due to fatigue or impact, parts must be cross-sectioned with little-to-no clear direction of where to make initial guess cuts. Figure 2 shows an example of a carbon fiber crank arm cross section that would be used to find defects. Vibrothermography is one solution to this problem. In vibrothermography, a test piece is vibrated at a high frequency (~20,000 Hz). This causes adjacent layers of the composite to rub if they are not well bonded to one another (e.g. if they are delaminated). This rubbing produces heat due to friction, and can be observed through an infrared camera. Dr. Chen has tested this extensively on rectangular, non-hollow coupons and shared his results with SRAM, a bicycle components company. SRAM is now interested in investigating the use of this method to discover defects in their composite crank arms.

A bicycle crank arm links the pedals of a bicycle to the bottom bracket (that is, the bearings in the frame that hold the crank spindle) and chainrings, providing power transfer from the rider to the wheels. Figure 3 shows the location of a crank arm on a bicycle. SRAM currently tests their alloy and composite crank arms to validate product lifetime, strength, and prove that they are abiding to standards imposed by the cycling industry. In these tests, the crank arms are cycled to failure, which is defined as crossing a threshold on the stress-strain curve, which varies based on the material. However, even after reaching this point in the test, it is often not possible to find the point of failure in the part non-destructively. While the failure is noticeable, the location of the failure isn't determined immediately, and finding it often consumes significant man-hours. Additionally, a nondestructive method of finding defects could one day be useful for other applications, such as warranty claims and quality control. Cutting the process time down from days and removing the destructive aspect can give SRAM a better means of engineering a solution to avoid failures.

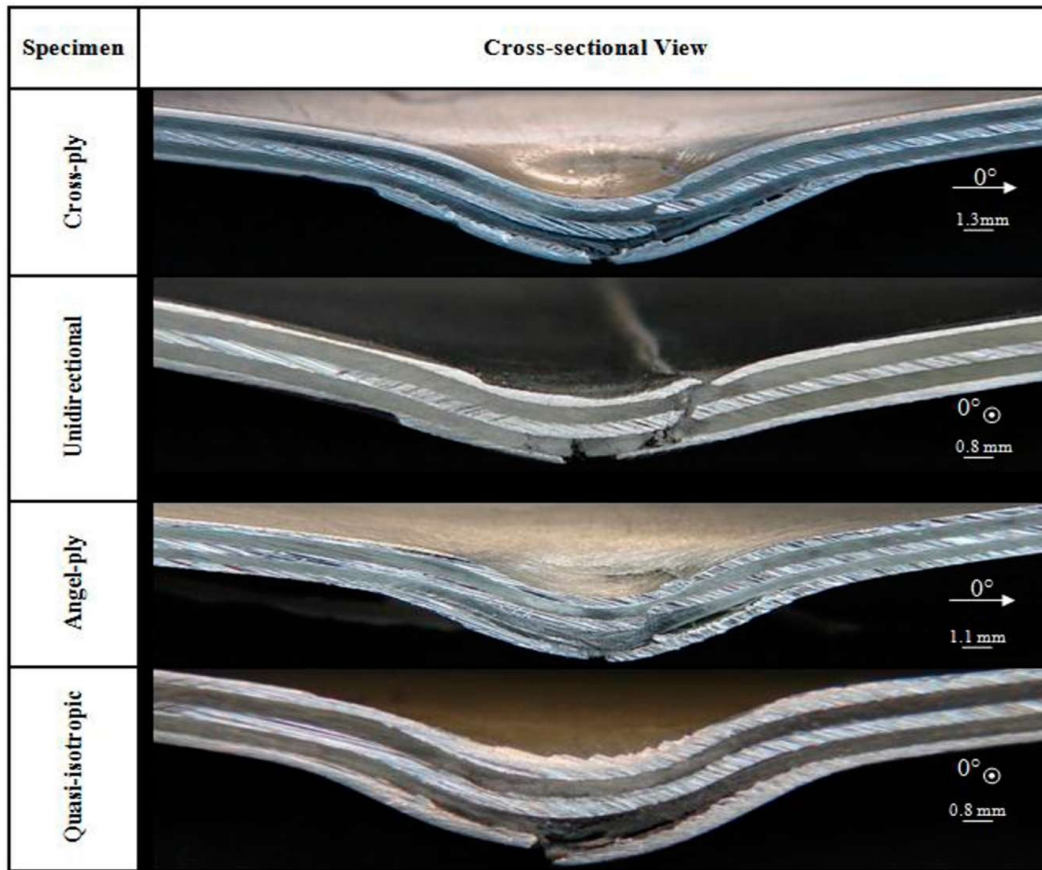


Figure 1. Several types of a composite laminate after impact testing. Though these are not carbon fiber, the damage, much like carbon fiber, becomes much more obvious in subsurface layers, making damage and defects very difficult to detect nondestructively [1].

SRAM hopes to utilize the vibrothermography testing format to find the defects and failure points in their crank arms more efficiently. In order to use this method, however, they need to verify that it is feasible with a crank arm, which is a more complex part than the rectangular panels that Dr. Chen has seen success with. We, the senior project team, will investigate this proposed solution and determine if vibrothermography is a feasible method for finding delaminations, flaws, and disbonds in the structure. In this feasibility testing, a SRAM Force crank arm, as shown in Figure 4, will be used as the subject to test for feasibility of detecting defects in the complex crank arm shape.

Team Management Plan

This senior project team was made up of Johnathan Simeroth, Grant Pocklington, and Tim Hoekstra, following a decentralized organization structure divided up by roles. Grant was the de facto leader and task manager, and oversaw manufacturing. Johnathan led reporting and analysis. Tim handled communications and records. Despite these loose titles, each team member was involved in every stage and every decision of the project. A specific delineation of the schedule that the team followed can be found in the attached Gantt chart, Appendix A.

II: Background

Carbon Fiber Reinforced Polymers (CFRP)

Most common materials (metals, glass, most polymers, etc.) are isotropic materials. This means that on a macroscopic scale, they have the same mechanical properties in every direction of the material. This is the result of a microstructure that has developed grains equally in all directions. However, another class of materials exists: anisotropic materials. Figure 5 shows a micrograph image that demonstrates the difference between the grain structure of isotropic and anisotropic materials. Carbon Fiber Reinforced Polymers belong to the class of anisotropic materials. This means that the mechanical properties (i.e. strength, elasticity, etc.) change depending on the direction in which they are tested. Therefore, an anisotropic material like carbon fiber may fail at a very low stress in shearing, or support no load in compression, but be very strong in tension, for example. This affects the way that parts using carbon fiber are both fabricated and analyzed.

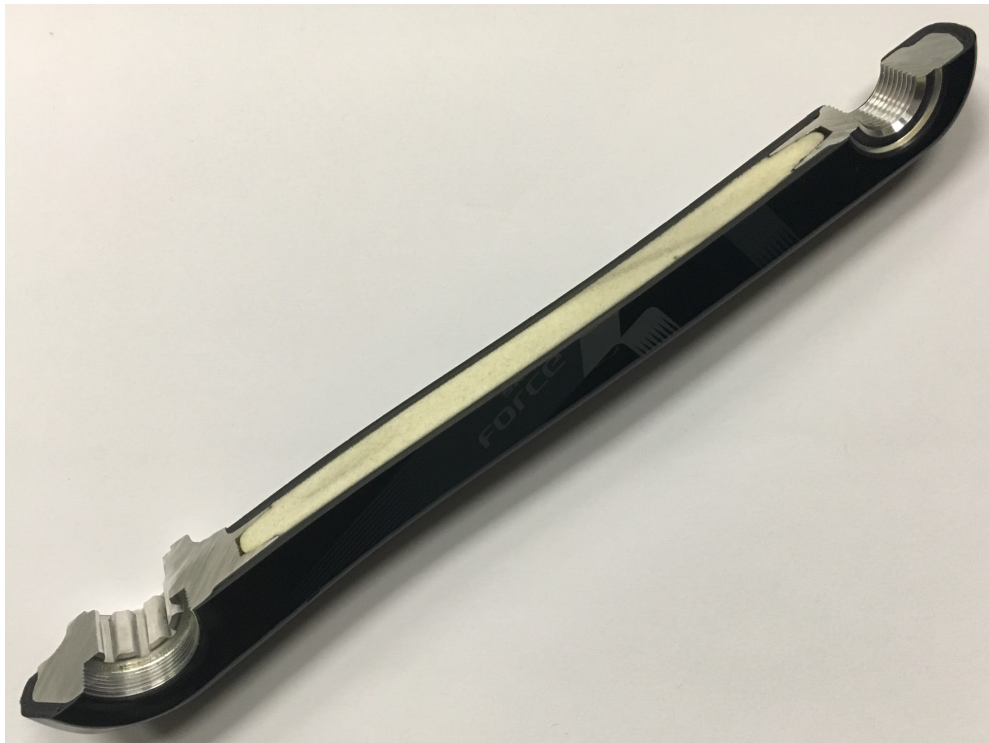


Figure 2. Cross section of a SRAM Force carbon fiber crank arm. Cross sections like these are made to find internal defects that are otherwise impossible to find.

Carbon fiber comes in different forms. These forms include unidirectional, weave, chopped, and milled fiber. As indicated by the name, unidirectional cloth is carbon fiber all following the same direction, which means it has very high tensile properties in the direction running along the fiber, and virtually no tensile properties across the fibers, as you can separate them entirely with ease. Weave is a combination of cloth directions, woven together. The fibers alternate in direction, which gives the cloth more uniform properties. Some variations of weave exist and may be specified by fiber count per weave. Unidirectional and weave are the most common fabrics used in the manufacturing of bike parts.



Figure 3. Crank arm location on a bicycle. A crank arm links the pedal to the crank, transferring power as the rider pedals [2].



Figure 4. A SRAM Force crank arm that we will be testing.

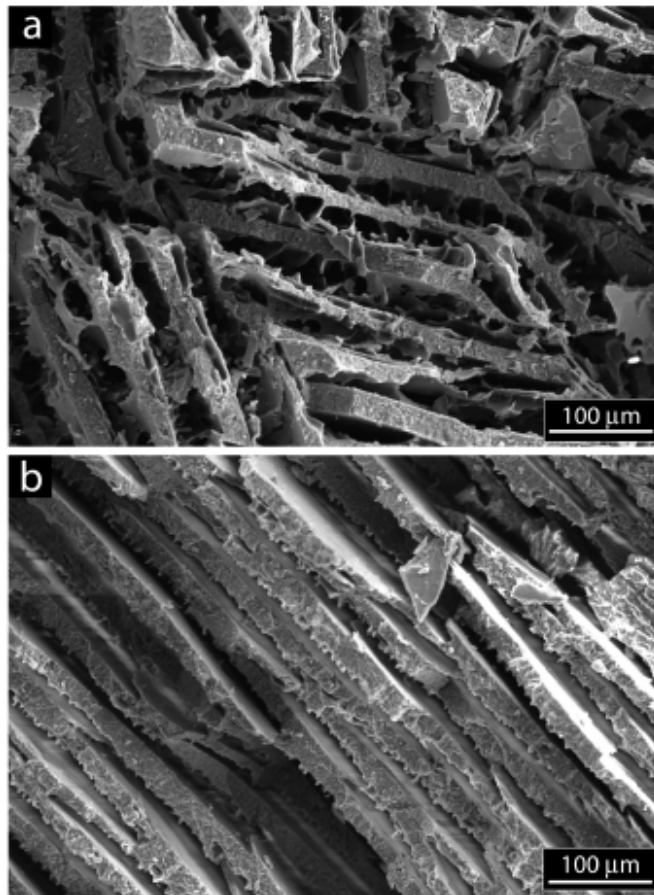


Figure 5. A micrograph of (a) an isotropic and (b) an anisotropic material. Isotropic materials have grains that grow in all directions, producing uniform mechanical and physical properties in all directions. Anisotropic materials' grains favor a direction of growth, giving the material mechanical properties that are direction dependent [3].

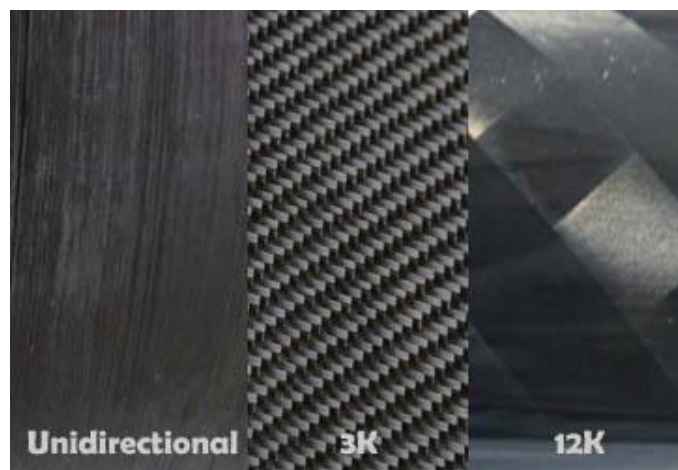


Figure 6. The visual differences between unidirectional CFRP, and two different fiber counts for woven CFRP [4].

A layup is the method by which carbon fiber is combined together in layers with different orientations and patterns and held together by a resin in order to create the desired mechanical properties of the final product. There are two types of fabric available that affect the layup process. The first type is standard carbon fiber fabrics with no resin in them. These are simply single-layer sheets of carbon fiber that must have an epoxy resin applied during the layup process. However, there are also fabrics that are pre-impregnated with resin, which takes some of the work out of the layup process because the laborer is no longer required to measure and calculate the proper resin density that is needed to fully saturate the carbon fiber layers and keep an even flow during curing. Both standard and pre-impregnated layup processes require a vacuum to be pulled on the fibers, to keep the resin from flowing in an undesirable direction and leaving a dry spot on the fibers post-curing. Some resins can be cured at room temperature, however many need to be cured at higher temperatures in systems like an autoclave or oven.

The mechanical properties of a layup are entirely based around which resin is chosen, what temperature the carbon fiber product will be used at (and therefore cured at), which kind of fabric is used in each layer, and how the different layers are oriented in the layup itself. The kind of fiber used, resin used, and the volume of the resin used determine the final weight of the carbon fiber product, as well as the overall mechanical properties. This tunability between weight and strength is a significant reason for the use of CFRP in many industries, including the cycling industry, where high strength and low product weight is an essential combination for competitive cyclists [5].

Vibrothermography, and Dr. John C. Chen's Procedure and Setup

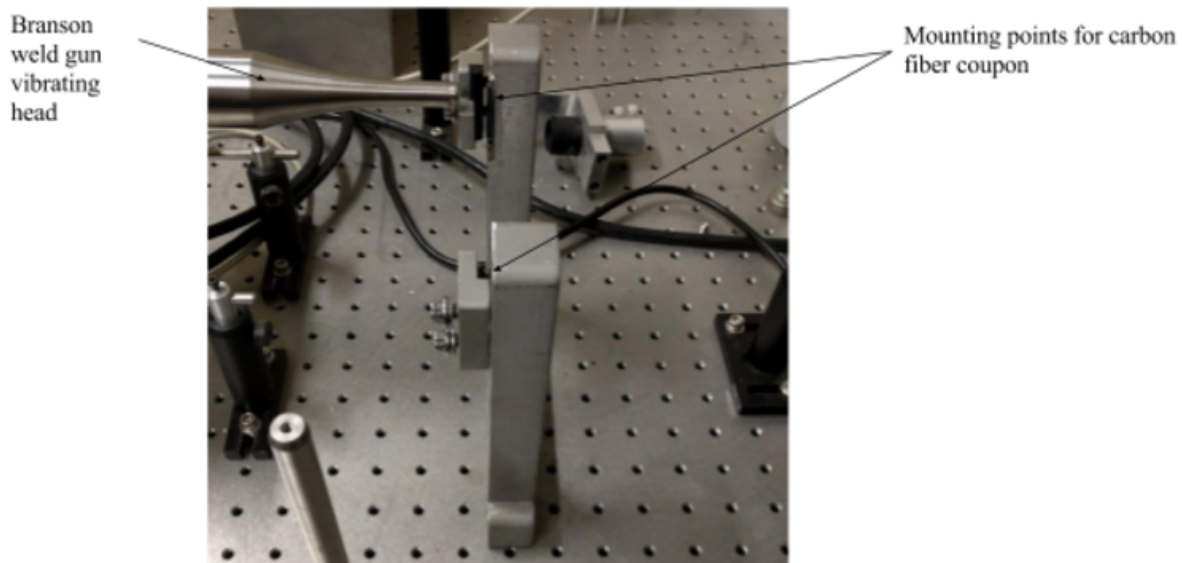


Figure 7. Dr. Chen's current fixture setup (side view) using 1" thick stainless steel uprights for holding the test pieces.

Vibrothermography, as we will use the term, refers to contact ultrasound testing using a vibrating source. This source vibrates at an ultrasonic frequency and is physically coupled with the test specimen [6]. In all of Dr. Chen's testing, he has used vibrothermography to detect defects. The equipment he has used to do this may be seen in Figure 7. This fixture is intended to allow maximum energy transfer to the carbon fiber panel.

In order to keep the vibrations transmitted into the part from being damped by the fixture structure and prevent damage and shifting, it is necessary to use some intermediate, non-metal material on the clamping faces. Dr. Chen used rubber with a cylindrical cross section at these interfaces in order to create a line contact with the test part when clamping it down in the fixture (see Figure 8). This allows the part to vibrate enough that the temperature difference between a normal surface and a delamination or other defect will be noticeable on the infrared camera when the part is being tested. This also prevents the clamping pieces from damaging the carbon fiber panel.

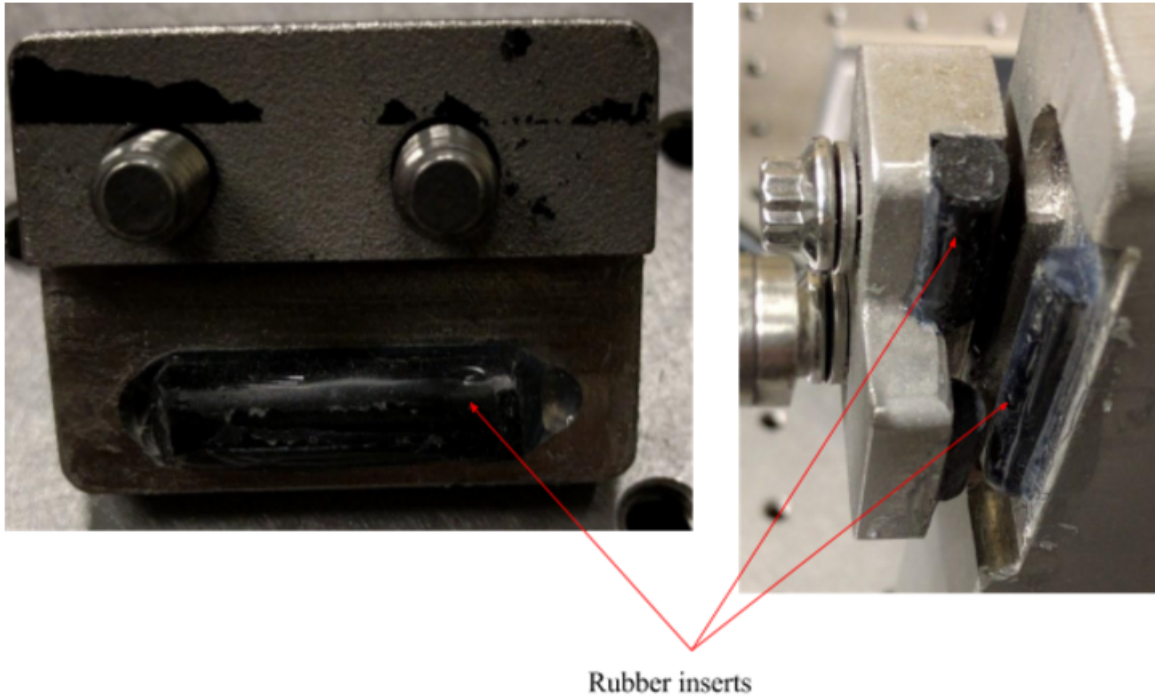


Figure 8. Close-up of part clamps with cylindrical rubber inserts

The Branson package weld gun shown in Figure 7 produces a frequency of 20 kHz. The gun is mounted on rails that allow motion only in the direction normal to the plane of the carbon fiber panel being tested. The tip of the gun is held in contact with the panel by force applied by a Clippard Minimatic CDR-24-2 pneumatic actuator with a bore diameter of 1.5 inches. However, to improve coupling and avoid damage, it is necessary to use an intermediate layer of duct tape, as shown in Figure 9. Many factors affect the results of this test setup. The pressure behind the weld gun, the torque to which the screws in the fixture are tightened, and the material used at the interface between the carbon and the weld gun are just a few examples. The gun must not remain activated for more than a couple of seconds, as the longer it is running the more heat is generated in the test piece. To avoid this oversaturation, Dr. Chen runs his test pieces for only a fraction of a second.

Until this senior project, the test pieces that Dr. Chen was using were simple carbon fiber panels that were prepared using different layups, and various kinds of defects. In some cases, he used a proprietary method to build in a delamination [7] that does not contaminate the piece with foreign materials. In other cases he dropped a known mass from a chosen height to create impact damage.

As depicted in Figure 10, Dr. Chen’s method could show the different depths of the delaminations based on how long it took for the heat signature to reach the surface of the plate, how large the defect implanted was, and where he had implanted it into the test piece.

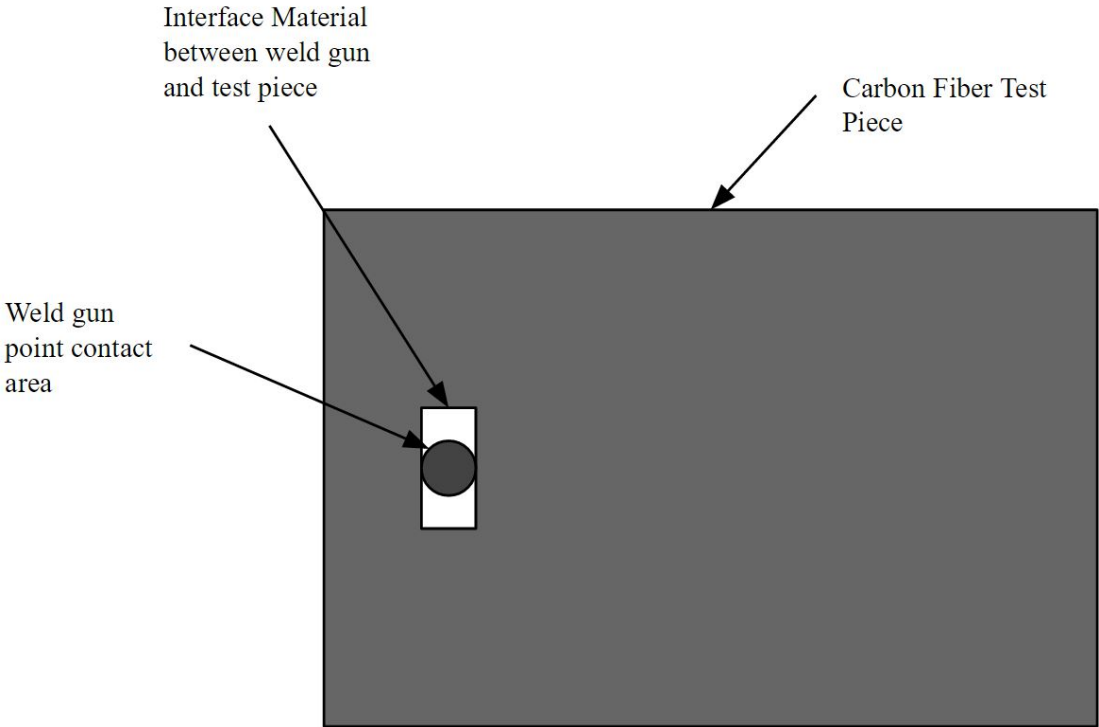


Figure 9. Standard carbon fiber test coupon with the duct tape interface material and gun location identified.

For some of Dr. Chen’s testing, there were slight issues with the implanted defects. If the defect was too large and the proprietary method resulted in a saturation of delamination effect, then the larger unintended delamination area would show up on the infrared camera after being vibrated. This was generally a flaw with the method of defect fabrication rather than with vibrothermography as a method of non-destructive testing (NDT).

Vibrothermography works best around the resonant frequencies of parts [7]. At resonance, the layers vibrate with the largest amplitude and generate more heat, which is how the defect is seen. The defects that can be detected by vibrothermography include impact damage, inclusions, voids, delaminations, and cracks. Vibrothermography can also be used in many applications when other forms of ultrasonic and radiography testing cannot output conclusive results [8]. There is also an added benefit of safety, as the infrared camera doesn’t need to be extremely close to the specimen that is being tested [8].

A limitation of vibrothermography is that it has a tendency to not illuminate any cracks that are parallel to the direction of the heat flow. Additionally, the change in fiber directions layer-by-layer can result in thermal property changes as well [8].

Thus far, the only method of NDT that has been covered is vibrothermography. However, vibrothermography is not the only NDT method of analyzing carbon fiber reinforced polymers. In order to understand other options, the alternatives are briefly discussed, including benefits and shortcomings.

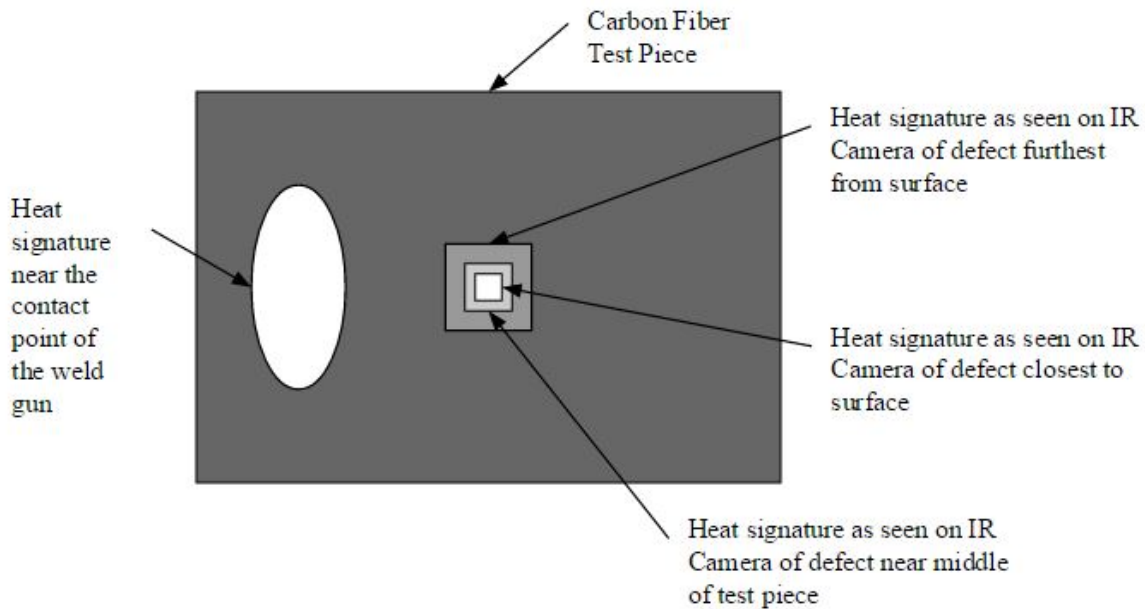


Figure 10. Depiction of a test piece with multiple defects at different depths that has been vibrated at 20,000 Hz, as seen through the Infrared Camera

Visual Inspection

Visual inspection is easily the cheapest method, and is quite functional for surface defects. Things like large sections of delamination can also be seen if they are near enough to the surface, however anything more than a couple of layers deep cannot be seen, and even smaller near-surface delaminations and cracks often cannot be seen. One solution to this problem regarding small surface cracks is to use a dye-penetrant test. In this test, dye is sprayed over the test piece and after some time is allowed for the dye to seep into fatigue cracks, it is wiped away. A developer (usually a white powder) is then applied to draw the dye out, which reveals locations of cracks [9]. Visual inspection is one of the current methods of locating defects at SRAM, however it is not useful or conclusive for defects and damage beneath the surface.

Laser Ultrasonic Testing

Laser Ultrasonic Testing (LUT) is a method of noncontact, or passive, ultrasound testing [10]. A laser may be used to excite the test specimen and generate ultrasonic frequencies. The major benefit of LUT, and most other non-contact methods, is that the results are not easily affected by distance or angle between the laser and the test piece. This is in contrast with contact methods where good coupling between the energy source and the test piece are absolutely crucial to successful test results. However, LUT is expensive, comes with safety risks inherent to laser use, and risks surface damage to the test piece [8].

Thermal Pulse Thermography

Thermal pulse thermography is a passive method of thermography that uses a heating element to energize the carbon test piece in a short burst [8]. The piece is then observed and recorded as it cools. A decrease in surface temperature with a non-uniform rate indicates defects [6]. This method has the benefit of not requiring direct contact to the surface of the test piece during testing. However, due to the simplicity of the test pieces used in most of the testing that has been published, it is unknown whether or not it will work for

the crank arm's more complex geometry and structure. Additionally, care must be taken to avoid damage to the surface of the test piece in this method due to the heat deposited onto the surface [8]. It is possible that this method can be accomplished with a high-powered heating lamp, which is generally less expensive than the ultrasonic weld guns used in vibrothermography. Per Sojasi et al., thermal pulse thermography detected defects with a little under 90% efficiency by the Tanimoto criterion, which is a ratio that considers true, missed, and false defect detections. This efficiency is one of the highest documented in Sojasi's paper [6].

Lock in Thermography

Lock in Thermography is another non-contact method of testing. This method uses a periodic—usually sinusoidal—heat source and an infrared camera with a frame rate that is synced to the wavelength of the source to measure and record test piece thermal response. According to Sojasi et al., “Internal defects change amplitude and phase of the [thermal] response signal on the surface,” [6]. This method, when paired with the right signal processing method, produced the best detection efficiency (by the Tanimoto criterion) at about 90%. Some of the benefits of Lock in Thermography are high accuracy, and high signal to noise ratio. However, this method also requires high precision calculations and significant programming. [11]

LED Optical Excitation

LED optical excitation uses, as the name implies, a Light Emitting Diode to excite the carbon fiber layers of a test part and elicit a thermal response. This method benefits from being low risk and comparatively inexpensive, but produces a low detection efficiency of about 16% compared to most other methods at 60-90% by the Tanimoto criterion. This is a result of the low energy input. LED excitation mitigates reflected radiation, but this is not enough of an advantage to compensate for the low energy input [6].

X-Ray Testing

There are two different types of radiography used for NDT of carbon fiber involving X-rays. The first of these methods is called conventional X-ray, which uses the standard radiation beam. This method involves flooding the carbon test piece with X-rays and using a film sheet backing to catch the level of radiation that passes through the carbon fiber. Areas that have a defect have a different appearance in the exposure, due to the varying amount of X-rays absorbed by the void or inclusion. This method often fails to detect low-depth defects (e.g. delaminations and cracks in carbon fiber) that occur perpendicular to the radiation beams. To solve this problem, X-rays may be taken at more than one orientation to increase the chances of identifying defects. However, this method is still insufficient for finding cracks, delaminations, and disbonds in a hollow crank arm. The cracks and delaminations would not be found with a single pass of the X-rays, and the hollow part of the crank arm would develop on the film backing as a void, making detection even more difficult.

The second x-ray method is penetrant enhanced radiography, which is useful for detecting defects with flaws that reach the surface of a part. The carbon test piece is covered in a fluorescent liquid and then it is left to allow the fluorescent liquid to penetrate deep into any cracks or defects that are present at the surface of the part. The part is then placed under X-rays. This illuminates any defect that the fluid seeps into when the fluorescent liquid shows up on the film backing. The obvious drawback to this method is that there needs to be a surface flaw for the liquid to seep into the carbon and matrix in order for it to be seen, which may not always be the case for carbon fiber crank arms [8].

III: Design Development

Requirements / Specifications

The final fixture design was a result of decisions on several different levels. The first level of decision making required a determination of which test format would be used. Therefore, before any further discussion occurred, we analyzed the various testing methods available. While there are many available options for the non-destructive test of carbon fiber parts, not all are equal. Some are lacking in their ability to detect the majority of defects. Others require test equipment that is simply not available or attainable for us at this time. Vibrothermography, however, produces results that are repeatable, visual, and achieved a high Tanimoto criterion efficiency rating of just below 65%. Though this is not better than Lock in or Pulse Thermography, it is still a relatively high efficiency rating, and demonstrates potential for success in testing, based on the success that Dr. Chen has seen in his experiments. Further, the equipment needed is available at Cal Poly, which means that delivering the project on time and within budget is possible with vibrothermography. We used a modified “House of Quality” tool to make this decision, and the results are shown in Appendix B.

With the first level of the test design decided, we could begin analyzing the needs for a specific fixture. The two most basic needs of any NDT test are that it shows defects, and that it does not damage the part. In addition, we recognized four basic categories of needs for a successful test fixture design:

1. Energy Transfer - how well the fixture allows for good coupling, and avoids absorbing large parts of the excitation energy. We consider this to be a function of:
 - a. Material at interface between part and gun
 - b. Material at interface between fixture and part
 - c. Type of contact geometry (area, line, or point contact)
 - d. Location of contact
2. Adjustability - how many different positions and forms the test fixture can take to allow for as many test conditions as possible. This includes factors like:
 - a. Part translation
 - b. Part rotation
 - c. Mount translation
 - d. Mount rotation
 - e. Base movement

This also affects our decisions about other factors. For example, we considered a design that allowed a material at the interface between the part and the gun to be switched out for a new material easily a benefit, because this allows for more variability of test conditions.
3. Visibility - how much of the part may be tested and “seen” by the camera. This is a function of:
 - a. Clamp solution
 - b. Part adjustability
4. Repeatability - how consistent we predict the results to be. We considered:
 - a. Number of fastened joints
 - b. Possibility of using locating blocks in a design
 - c. Limiting the number of possible orientations

We considered these four categories in designing a test that could determine the feasibility of detecting failure in carbon fiber crank arms using vibrothermography.

Upon discussing the engineering specifications and house of quality, we noted that most factors have a positive correlation, so improving one of them improves the others as well. However, for the fixture design, more parts of the fixture might negatively impact detection efficiency because more parts on a fixture means less rigidity and repeatability. Therefore, we expected the final fixture to be a balance of versatility (gained at the cost of additional parts and complexity) and rigidity/repeatability.

We also strongly considered safety while developing a design. However, most of the designs promote a near equal level of safety. The greatest risk in this project was in manufacturing, which was addressed in accordance with Cal Poly's shop safety standards.

Concept Generation

Several methods of brainstorming were used in the early stages of this project. We began by generally listing and describing different concepts and ideas we each had. Once we had a few ideas for most of the parts of our project, we realized that looking at everything together was not the best way to accomplish this task.

Moving forward, we brainstormed each section of the project independently. These were separated into three categories: method of energy transfer into the part, part mounting, and part clamping. We brainstormed for each of these categories individually, using methods like Brain Writing and Scamper. In each of these categories we recorded as many ideas as we could and then filtered them based on feasibility of implementation, machinability, and expected utility. We also included and considered ideas that Dr. Chen has already been testing and noted what worked for him, and what didn't work. These weighed heavily on our final decisions.

Idea Selection

To organize and down select the numerous concepts and solutions generated, we developed a structured way to evaluate the degree to which each solution fulfilled our design goals. Our overall design goal was fixture versatility - the ability to vary different aspects to find a successful detection method. To evaluate various concepts in meeting design goals, we named four categories: energy transfer, adjustability, visibility, and repeatability. In each category, we defined possible ways of fulfilling the goal and ranked each individual concept in how many ways it allowed us to fulfill the goal, giving us a ranking of which concepts would give us the greatest chance of meeting all of our design goals and ultimately, fixture versatility. Table 1 shows these different solutions methods and the evaluation criteria for each, as well as the four overall design goals.

Table 1. Summary of fixture design goals and solution paths. In italics are concept evaluation criteria.

Design Goals	Solutions	
Energy Transfer	Material at interface	<i>want to vary</i>
	Type of contact (geometry)	<i>good or bad</i>
	Location of contact	<i>want to vary</i>
Adjustability	Part slide	<i>possible?</i>
	Part flip	<i>possible?</i>
	Mount slide	<i>possible?</i>
	Mount flip	<i>possible?</i>
	Base movement	<i>possible?</i>
Visibility	Part adjustment	<i>possible?</i>
	Clamp solution (blocking)	<i>good or bad</i>
Repeatability	Limit orientations	<i>good or bad</i>
	Locating blocks	<i>possible?</i>
	Number of fastened joints	<i>good or bad</i>

We elected to divide the fixture design into three somewhat independent “modules”, allowing us to choose the best concepts for each module to be combined in the final design. For each module, multiple concepts were generated and evaluated against each other. The first module was clamp solution and describes the way the crank arm will be held, clamped, and the interface material to be used. The second module was the mount solution, describing the way the clamped part is attached to the base, located, and adjusted. Finally, the third module was the base solution, how the mounted part would be fixed to the table. Each module was evaluated separately, in order for the best parts to be combined in a final fixture design.

These evaluations of each concept were organized in a matrix which can be seen in Attachment C. The results of the idea selection showed that a line contact or v-block clamping solution would give the most versatility in testing. In addition, a slotted plate mount on a base with two uprights would compose the remainder of the fixture.

In addition to on-paper brainstorming and concept generation, we elected to include preliminary testing in our fixture design process. To augment and inform our decisions on a final fixture design, we wanted to complete some rudimentary testing with a simple, quick fixture to gain an understanding of what would be needed in a more formally designed fixture. As a rough, first-pass design, we kept this fixture simple and used a clamp design (Figure 11(a)) that allowed us to get a baseline test. This baseline testing was done with the setup that Dr. Chen had been using. Based on the results of this preliminary testing, we adjusted our design for the next fixture.

Initial testing with this first fixture informed our design decisions and helped us understand better the needs of a final fixture. The testing showed that even without fine-tuning any testing parameters, the testing method showed potential. We were able to see major defects in the tested parts using the first fixture (further discussion can be found in the results and analysis section). This fixture showed that the pressure of the gun is sufficient to hold the test piece in place, and it is unnecessary to clamp the part in the fixture in most cases. In fact, clamping with significant pressure deadens the vibration of the part. The initial testing

indicated that was better spent adjusting testing parameters before creating a new fixture - the first fixture was adequate for this portion of the testing.

IV: Description of the Final Design

Design Development History

Testing with the first fixture gave results that indicated presence of defects in the parts between the two aluminum lugs. With the first results promising, we spent more time honing our testing parameters and demonstrating feasibility using the first fixture.

During this time, we created plans for a second fixture based off our initial concept generation and learnings gained from testing in progress. This fixture would increase adjustability and modularity for different mounting solutions. This design was refined to eliminate unnecessary complexity by removing components and integrating their function into the upright structure. The design had a U-shaped base with a slot to attach to the table, and an array of threaded holes for attaching almost any clamping solution. Two clamping solutions were considered: a line contact geometry, similar to our first fixture, and a cantilevered rigid spindle attachment. The total cost of materials and tooling for the manufacture of this fixture was approximately \$500. A more detailed cost report is included in Appendix F.

The U-shaped base had a slot in the bottom for a single screw to attach through to the table. This design allowed for rotation of the whole fixture in the plane of the table, as well as a degree of freedom for translation along the direction of the slot by only loosening one screw. To add rigidity to the fixture, toe clamps would be used as a simple, quick method of rigid fastening in an infinite number of positions by utilizing the feet on the sides of the fixture as seen in Figure 12. The ability to translate as well as rotate should remove the need for shim plates to account for the offset. This freedom should make it possible to contact the crank arm in several different locations, while maintaining the contact surface normal to the gun axis.

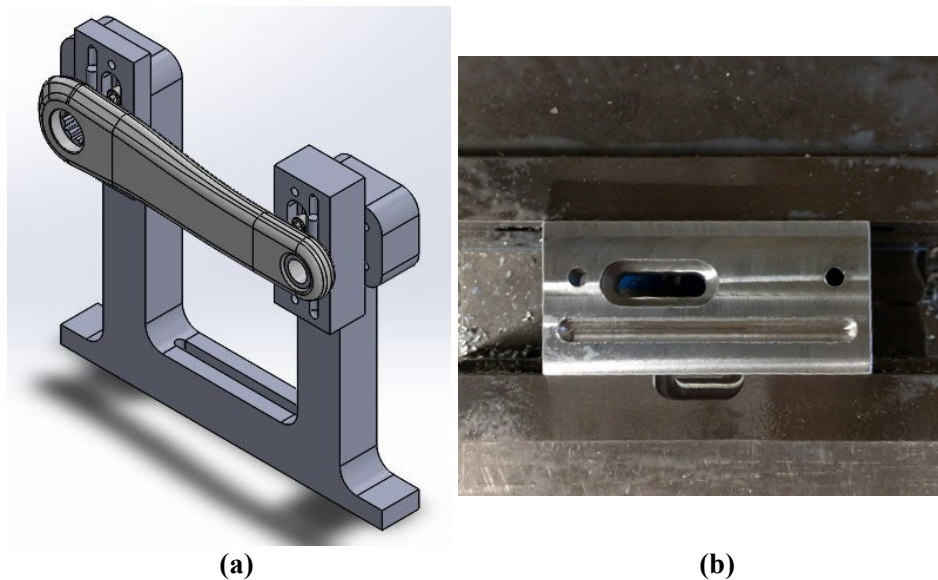


Figure 11. (a) Fixture concept showing U-shaped base with two mounting blocks. The tabs located on the bottom are locations for two toe clamps. **(b)** As-machined backing block

The design also allowed for multiple mounting solutions to be used in various configurations. An array of threaded holes on both vertical lengths of the U provided locations for mounting hardware to be attached. This hardware could be moved to support the crank arm in a variety of locations.

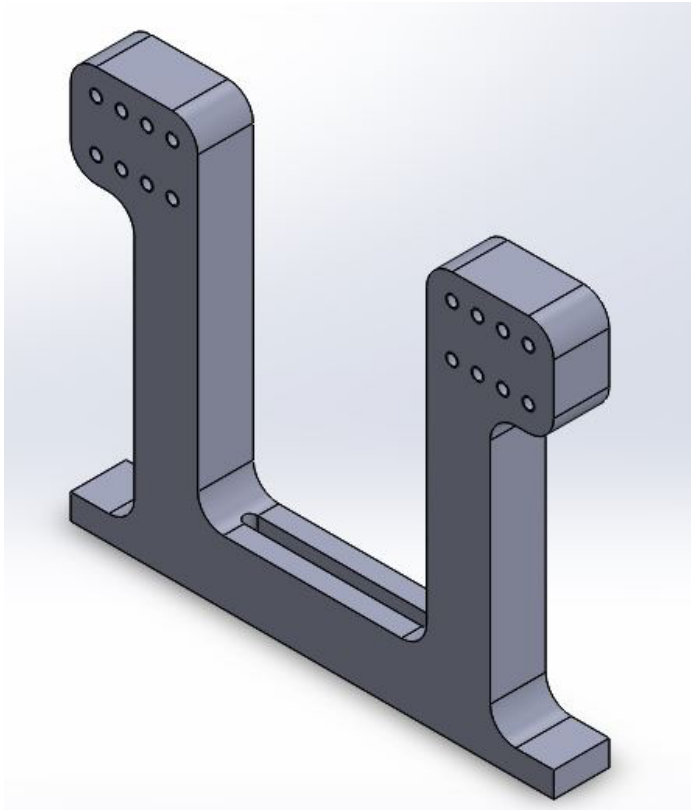


Figure 12. U-base showing mounting hole array on upright sections and single bolt table attachment slot.

We developed concepts for two such mounting configurations. The first configuration was a set of blocks that provided line contacts to support the crank arm on either side depicted by Figure 11(a). As seen in Figure 11(b), with the use of slots, we were able to make these blocks work with both the existing and proposed uprights, which allowed us to test them immediately. These backing plates were also designed and machined for the SRAM Force crank arm’s offset to allow for the gun to contact the crank arm normal to the surface at the point of interest of our initial tests. These blocks could be adjusted in and out so that the crank arm was simply supported with a varying span. The crank arm would be held in place by the pressure of the gun - initial testing showed this to be a convenient and favorable way to constrain the test piece, and better results were seen from the increased freedom of vibration gained from not rigidly clamping the test piece. The outer face clamps could still be used if a different holding method was being tested.

The second mounting configuration involved rigidly attaching the crank arm to the U-base by means of an actual spindle section welded to a small plate (see Figure 13). This spindle carrier plate uses slots for mounting to the existing upright allowing for vertical adjustability. This cantilevered configuration was inspired by observation of typical crank arm fatigue testing. Mounting the crank arm in this fashion would replicate the fixturing that SRAM is utilizing for their fatigue testing. With feasibility proved in this mounting scenario, this method of defect detection could be readily adapted to current fatigue testing regimens with parts being tested in situ.

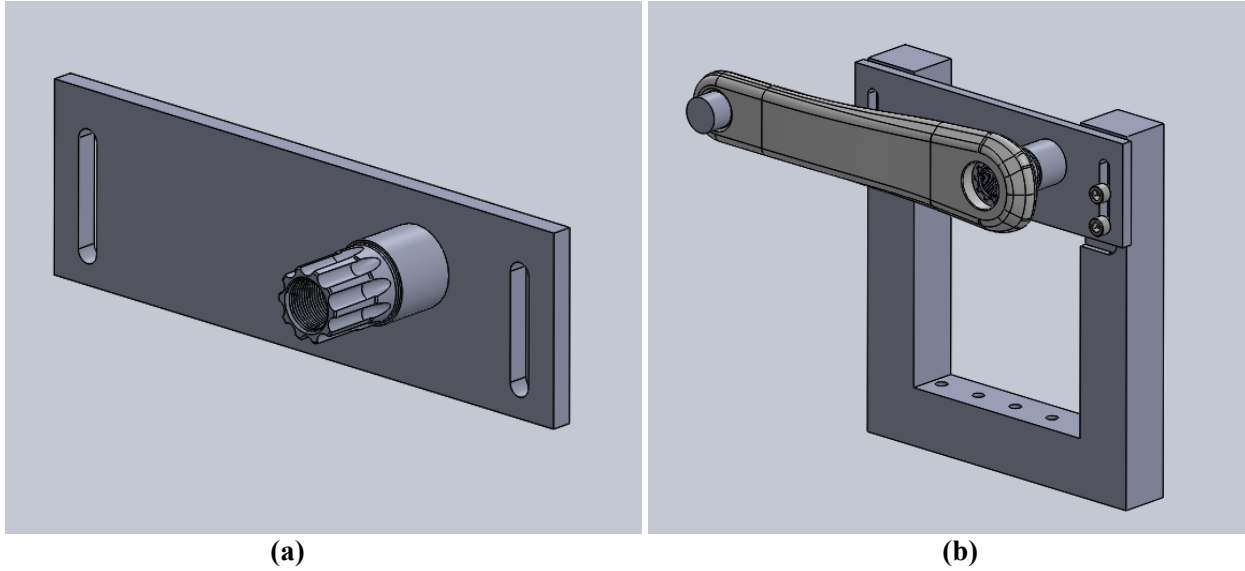


Figure 13. (a) Rigid spindle mount weldment. (b) Fixture concept shown using the rigid spindle mount. The pedal side of the crank arm is unsupported and an optional plug (shown) provides an additional gun interface location.

In our analysis for this design, we wanted to ensure that the fixture would not resonate near the frequency of our ultrasonic excitation, absorbing the energy of the test. During crank arm testing, the input vibration is at a frequency of 20,000 Hz. To prevent strange anomalies in the testing, we looked at the frequency analysis of a simply modeled upright structure to make sure the structure was not going to be operating at a natural frequency. The 28th natural frequency (shown in Figure 14) operated near the 20,000 Hz at 20258 Hz. This should not create issues with our testing, because in addition to being 258 Hz from the input frequency, the resonant vibration will have a negligible magnitude at such a high mode.

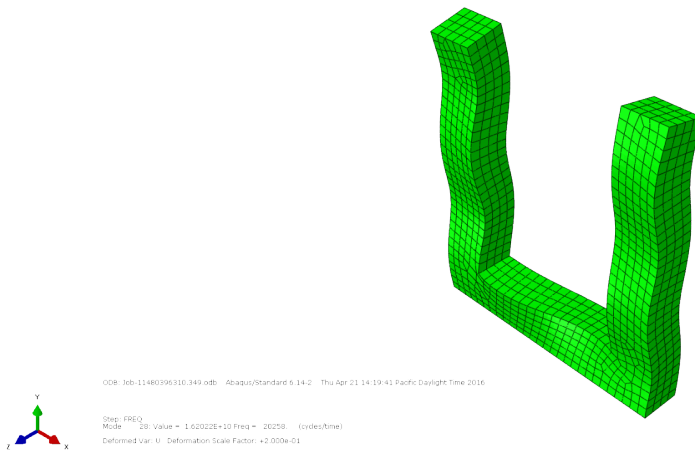


Figure 14. FEA frequency analysis image at the 28th natural frequency, which occurs at 20258 Hz

When modeling the simple U-shape structure in Abaqus, the two pockets and two holes on each of the vertical sections were neglected to simplify the mesh, as were the mounting holes for the fixturing at the base. The model was constrained along the entire bottom surface, which is an approximation of how the

upright is affixed when under use. The elastic modulus used was 28500 ksi, with a Poisson's ratio of 0.29 to model the structure's material. The model was dimensioned from nominal dimensions of the existing upright.

This analysis was highly simplified and constrained to only the structure of the U-shaped upright. There are barriers between the crank arm, where the energy is being input, and the upright itself, that further complicate the actual frequency that is seen by the upright and how the mass and energy input is distributed.

Final Design

Although adjustability in a test fixture was a high priority, we decided to explore a low risk parallel path with potentially high rewards. With only a few hours of machine time, we manufactured a test fixture that very closely replicated the fixturing that SRAM crank arms are secured in during fatigue testing. This fixture did not allow for a high level of adjustability, but it did save us from machining a new upright. Proving the feasibility of the test under these circumstances was the best-case scenario, because SRAM's ideal test would be one that they could implement directly into their existing process.

To further replicate SRAM's current testing setup, we assembled the cantilever fixture with one half of the bottom bracket, allowing the clamping force to preload the bearing, as SRAM would have done for their fatigue testing.

In addition, this design utilized the cantilevered mounting concept, which we thought might be a better method for transferring energy into the crank arm, rather than damping the input against rubber supports. The manufactured fixture can be seen in Figures 15 and 16.

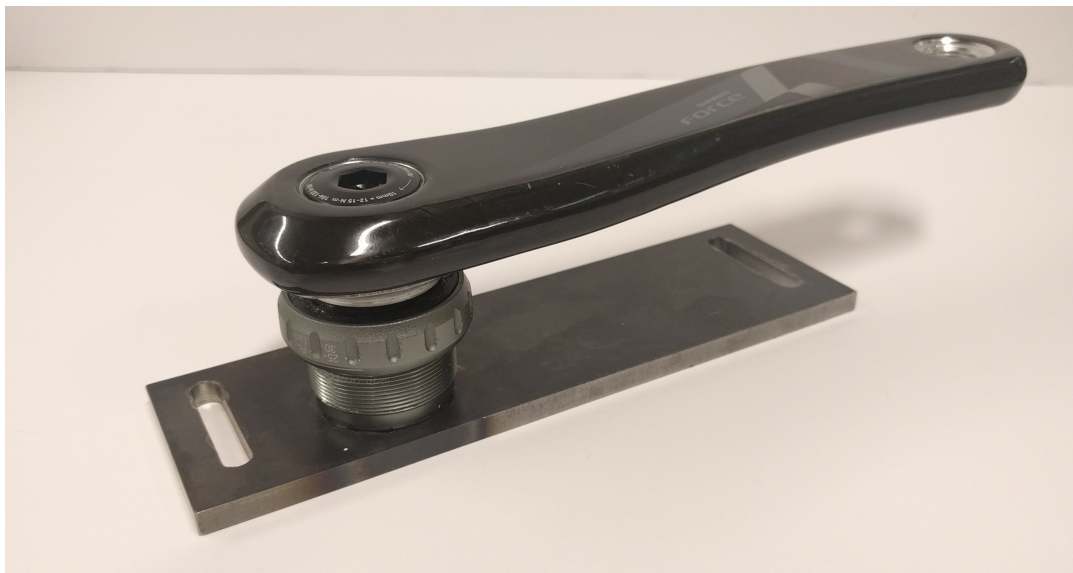


Figure 15. Final fixture mount design assembled with the bottom bracket (light grey) in place and the crank arm mounted.



Figure 16. The final cantilevered spindle mount fixture shown with a crank arm installed without the bottom bracket.

Testing with the spindle mount fixture was very successful (see VI: Results and Analysis). As a result, we elected to make this fixturing method our final design, rather than the more complex and versatile fixture.

V: Testing Information

Test Plan

Unlike many of the senior projects, this project had a much stronger emphasis on testing than on any other aspect. This is because the purpose of the project was to determine if testing crank arms with vibrothermography produces reliable results.

Unfortunately, the indicators of a successful test are very qualitative, and hard to quantify. Traditionally, two qualitative indicators have been considered: the sound produced when the gun excites the part, and the image produced by the infrared camera. In Dr. Chen's testing, a successful test is indicated by a high-pitched screeching sound emitted from the vibrating test piece. Additionally, the infrared camera picks up a very clear temperature difference at the location of the defects. However, our testing revealed that the screeching sound is a function of test specimen shape. Dr. Chen's rectangular panels resonated well and produced this sound, but the crank arms did not - even when the test was successful. This left us with only one indicator of a successful test: whether or not defect locations could be correctly identified.

To make the best use of our time testing, we established a list of parameters that would likely have the greatest effect on our ability to see a defect. In order of importance, these variables are:

1. Total energy input (this is a setting on the weld gun controller)
2. Pressure behind weld gun
3. Clamping configuration (i.e. whether the crank arm is clamped on both sides or only one, whether it is clamped at all or simply pinned between the pressure of the weld gun and the back of the clamp, the positions of contact between the clamps and crank arm, etc.)
4. Gun placement (where the gun is contacting the crank arm)
5. Tape (layers and replacement interval)
6. Rubber durometer

The tests followed an OFAT (one factor at a time) testing method. That is, we determined initial values for all the variables, and held them all constant while varying one of them over a range. Because we identified what we expected to have the greatest impact on test results, our plan was to begin by varying the most significant variable, energy input. After varying it over a range and recording the results from each run, we expected to find that the maximum amount of energy we could input without damaging the part would give us the best results. Once that variable was set, we planned to alter the pressure behind the weld gun over a range, recording each run. We would then change the clamping configuration, and run through the same series of variations in gun pressure. We would repeat this procedure until we determined the optimum combination of variables. More details may be found in the attached test plan (see Appendix E).

Testing was evaluated qualitatively, by comparing images to each other and judging which parameter value yielded the best images for detection of defects. One anticipated difficulty was the buildup of latent heat in the part after repeated testing runs. This “saturates” the image and makes it more difficult to distinguish hot spots that are generated. However, with the correct testing parameters, the defects were illuminated so clearly that this was not an issue (see VI: Results and Analysis). An additional concern was that cumulative damage from the weld gun tip and variability in the taped contact region from run to run would make it difficult to clearly differentiate the effects of varying each parameter from the testing “noise”. Again, however, this proved to be a non-issue as we began to see how clearly the defects lit up, and how clearly certain parameters changed these results.

Control Testing

To understand what is and what is not a defect, we had to establish a baseline from out-of-the-package crank arms. From these tests, we were able to see that the foam section on the inside of the crank arm produced a heat signature, as shown in Figure 17. This heat signature was in all of the tested crank arms, and was ignored if there was no other indication of a defect in the region.

We also tested a crank arm that had inflicted damage from the round side of a ball peen hammer to see what sort of heat signature that would produce along the area where the foam insert was. This imposed defect was discernible from the standard heat signature that was seen in the out-of-the-package crank arm testing.

With these tests completed along a series of gun pressures and orientations, we felt comfortable moving on to the fatigue tested crank arms with defects to explore what parameters would best indicate a defect around the areas of interest.

Optimized Testing Parameters

Despite being our number one factor, total energy input proved to be impossible to alter in practice with our equipment due to a broken set of buttons on the controller. However, this did not prevent us from achieving successful tests (see VI: Results and Analysis).

We tested at a range of cylinder pressures from 5 psi to 20 psi (which, for our 1.5” bore diameter, equate to 8.8 lbf and 35.3 lbf of contact force, respectively). We found 17 psi (30.1 lbf) to generally give the best results and chose to do most of our testing at this pressure. We did not exceed 17 psi for much of the testing to avoid damaging the crank arms and other test equipment.

We attempted multiple clamping configurations, but the most successful method was the use of the spindle as a mounting point (i.e. the cantilevered mounting method). In addition to providing the best excitation results, this also made for a highly repeatable test setup because each crank arm was located by the fixed position of the spindle mount.

Several locations on the part were tested to observe the effects of gun placement. However, this factor - as predicted - did not prove to be very significant so long as the weld gun was contacting the carbon fiber surfaces. The one thing that we were able to determine from this testing was that contacting a metal part directly - e.g. a plug threaded into the pedal spindle as shown in Figure 17 - did not work. We were disappointed to discover this because contacting a plug in the pedal spindle would have been a very convenient way to test parts and would have guaranteed that no surface damage occurred at the contact point. However, infrared (IR) footage revealed that most of the energy input to the pedal spindle plug was quickly dissipated through the surface of the plug and into the mating threads in the spindle. We saw similar results with the spindle lug threads when using the cantilever fixture as well.

We attempted tests with different numbers of layers of tape, but these proved to do little to nothing to the test results. However, we did learn that replacing the tape regularly (i.e. with each run) was key for reducing damage to the surface of the crank arm. An increased number of layers also had this effect, but marginally by comparison.

Finally, harder durometer rubber (90 shore A) gave slightly better results than the softer rubber that we tried (60 shore A). The results were very minimally affected by this parameter, and we therefore did not invest any more time experimenting with other durometers of rubber.

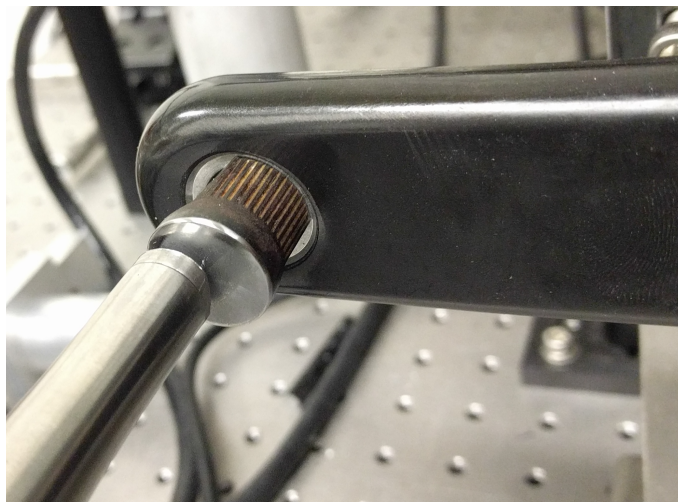


Figure 17. An unsuccessful method of gun placement that would have avoided surface damage during testing.

VI: Results and Analysis

Testing results indicate significant capability for detecting defects in carbon fiber crank arms using vibrothermography. Following is a discussion of our test results and the techniques developed for interpreting and viewing the infrared image capture, showing the test data from a crank arm damaged with a ball-peen hammer in the midsection.

Image Analysis

Data is received from the infrared camera as a series of still frames in grayscale, with each shade of gray correlating to a different temperature value in the range of values present in each frame. However, differences are very difficult to see in this format (Figure 18).

To enhance the temperature differences in the image and make it easier to interpret temperature, we adjust the dynamic range of the images to increase the contrast (i.e. set the darkest gray as “black” and the lightest gray as “white”), shown in Figure 19a, and then assign a different color to each gray value to create a familiar colorized representation of temperature (Figure 19b). After this step, it is already easy to see which parts of the test piece are warmer and which are cooler. There is a significant hotspot that forms near the gun, as well as hotspots where shiny portions of the test setup reflect radiation from the surroundings.

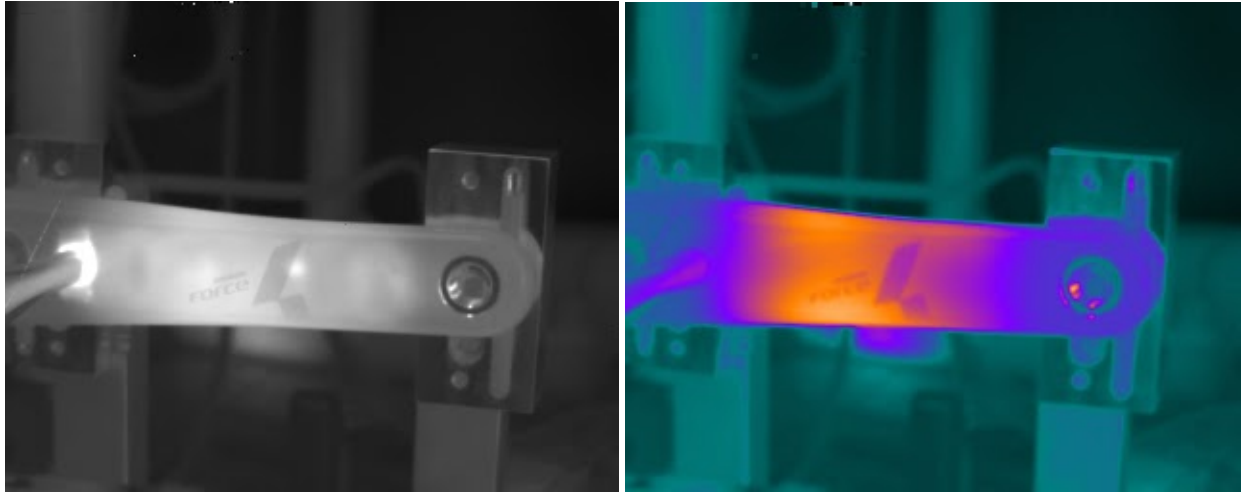
However, what we are most interested in is the change in temperature throughout the test. Vibrothermography causes defects to heat up during testing and this is what we want to focus on. In order to highlight any changes in temperature, we can subtract the first “resting state” baseline image (Figure 20) from each image in the sequence, essentially “zeroing” each pixel. After this step, any pixel that does not show a temperature change remains black and hotspots are more apparent. An example of this is shown in Figure 21, showing multiple hotspots and a likely defect in the center on the logo.



Figure 18. Raw image data from excitation of crank arm with hammer punch defect ($t = 0.1s$)

All of this image processing can be completed in imageJ, an open-source program mainly used in biology and cell counting. Macros can be written to systematically process large sets of data and many user-created plugins exist for a multitude of applications. If testing setup allows for highly repeatable and comparable results, the program can even be configured to run quantitative analysis of the gathered image data. Processed image sequences can be exported in a variety of formats, including .avi and .gif files.

The use of a macro replicating this process will allow us to quickly view and interpret our test results, even during testing sessions, and aid us in presenting any findings. Using these methods, even subtle differences in the gathered data can be magnified to highlight any temperature changes and allow us to better compare the results of different test parameters and fine-tune the testing to maximize detection.



(a) **(b)**
Figure 19. (a) Image at $t = 0.1\text{s}$ adjusted to increase contrast (b) Initial frame showing pre-excitation state ($t = 0\text{s}$), with color mapping. Orange indicates hotter areas. Overall heat difference shown is on the order of 1-2 degrees or less.

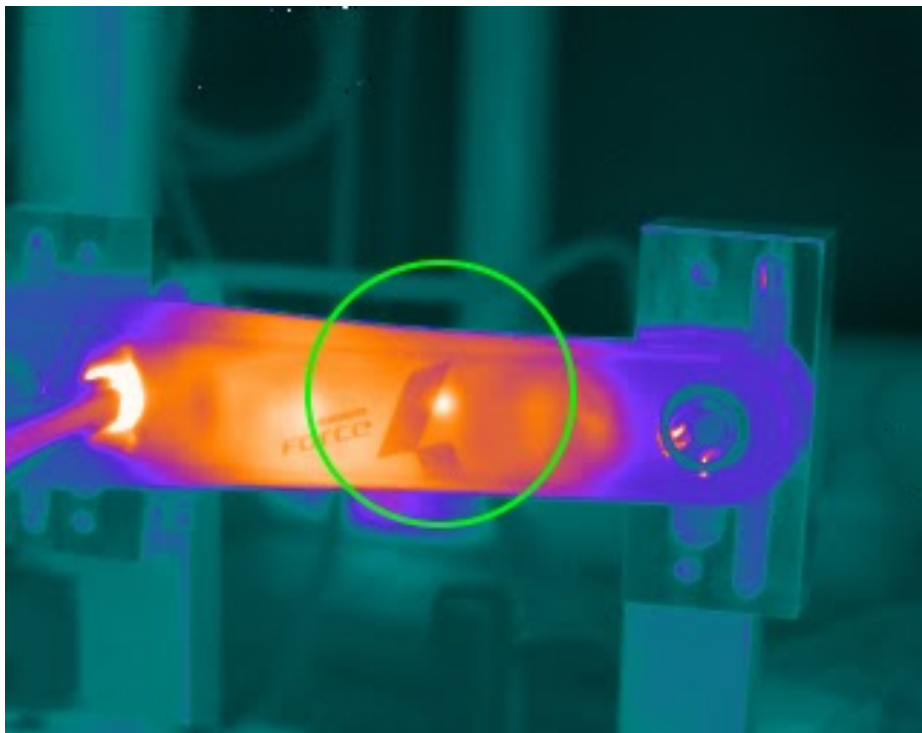


Figure 20. Color mapped image at $t = 0.1\text{s}$. Location of defect denoted by green circle.

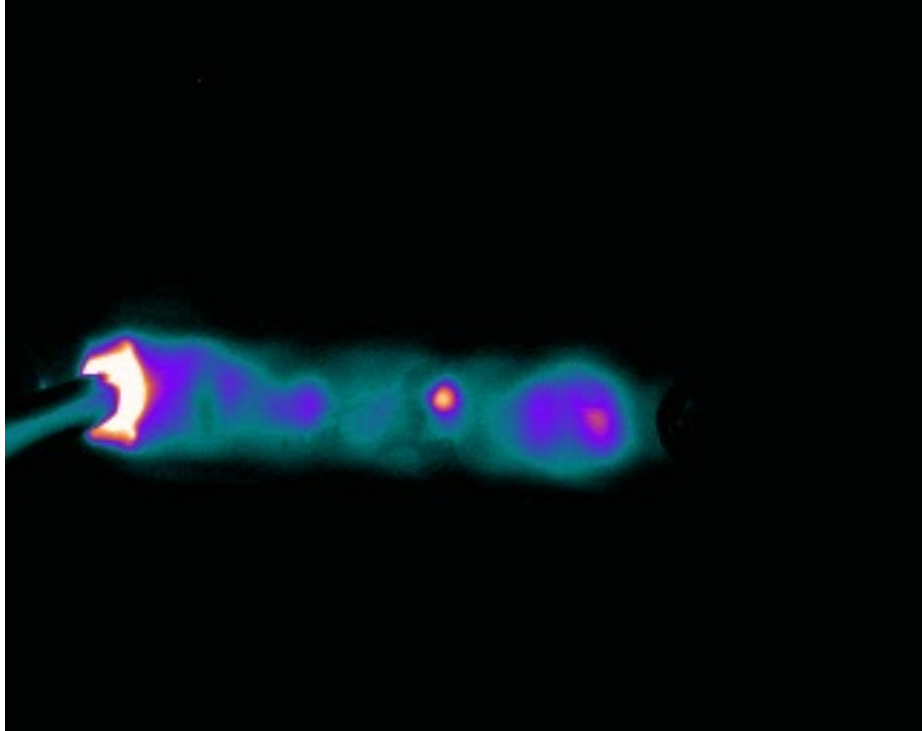


Figure 21. Image at $t = 0.1\text{s}$ with initial baseline frame subtracted. Black areas indicate no change in temperature during testing. Defect in center is apparent.

Although in this case the defect was highlighted by this method of image analysis, there is some risk of creating false positives through this image analysis. In addition, for small defects like the one shown in Figures 18-21, the temperature difference is so low that even the standing waves created by the weld gun in the part are highlighted, which could lead to confusion. This is less of an issue when the defects are more obvious, as shown in Figure 23.

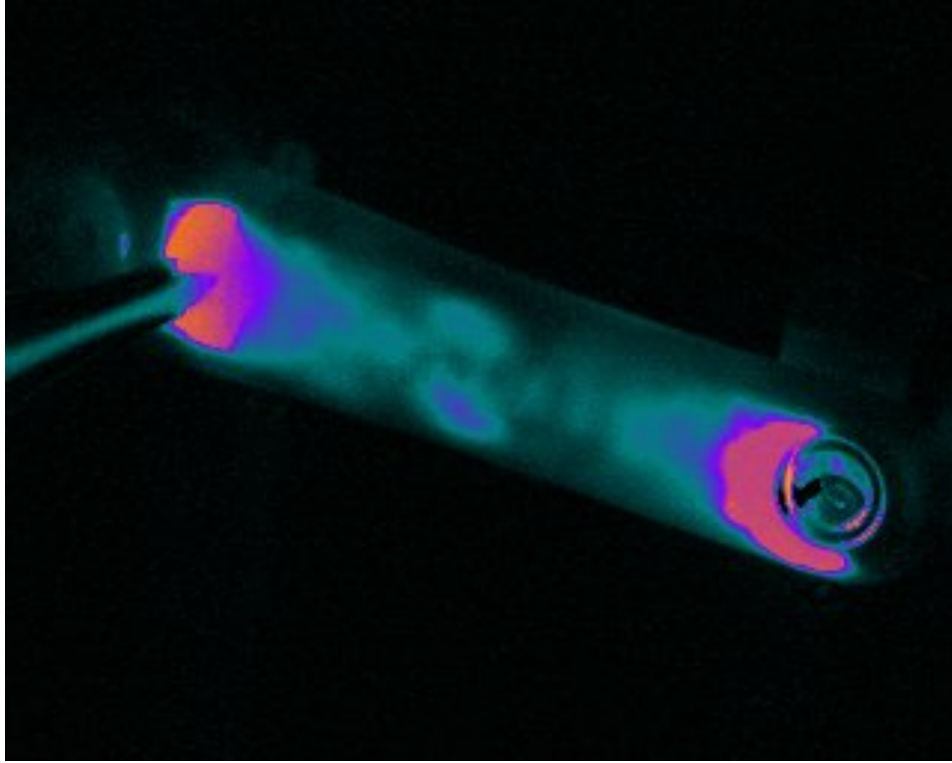


Figure 22. Image at $t = 0.1\text{s}$ with initial baseline frame subtracted, showing large disbond between the aluminum lug and carbon fiber near spindle mount.

Results

Figure 24 shows one of the images of the testing performed with our optimized parameters and our final test fixture. This figure shows the very clearly highlighted section near the pedal spindle. Repeated testing on this part and a number of other fatigue damaged parts showed a very similar location for defects with each test. Further, SRAM verified that this location is precisely where they expect to find defects due to disbonding in this fatigue test.

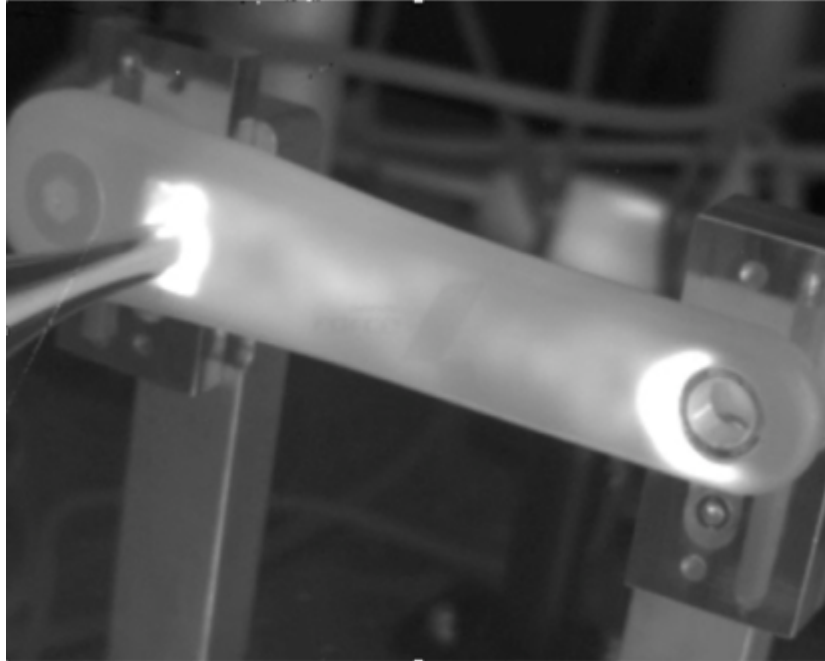


Figure 23. A very clear disbonded area can be seen around the pedal spindle (right). This defect formed a crescent shape, starting closest to the pedal spindle insert, and radiated outward. Crank arm F9731

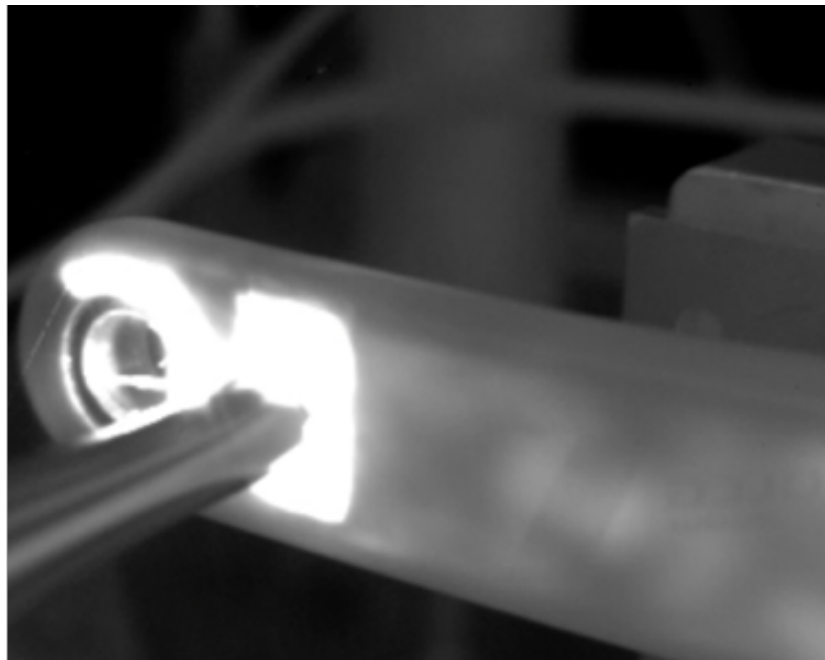


Figure 24. The same defect as shown in Figure 23. Gun placement in these two positions shows that gun placement has very little effect on the visibility of the defect. Crank arm F9731

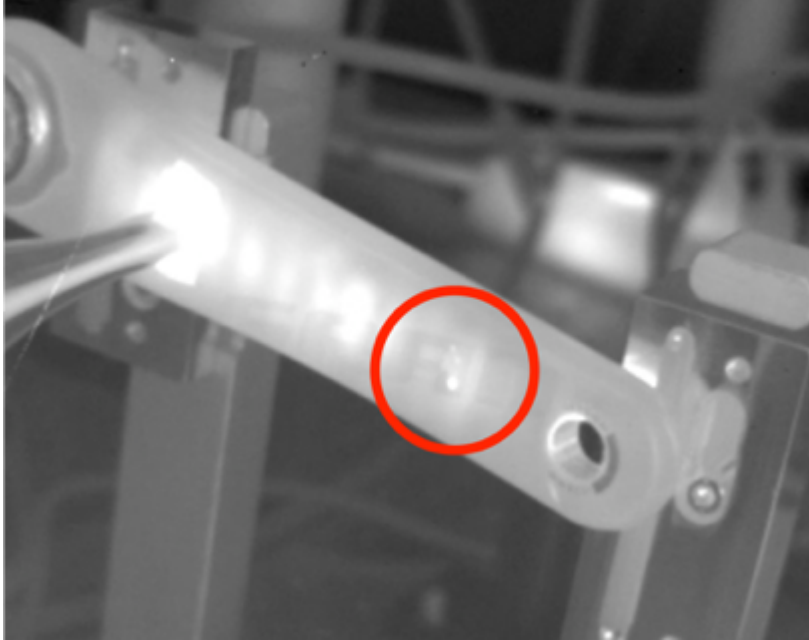


Figure 25. A highlighted spot of a previous test location reveals that the test may not be entirely non-destructive. Crank arm F9738

VII: Conclusion

We have determined that vibrothermography is a valid method of nondestructive testing for carbon fiber crank arms. In our testing, it reliably detected and revealed the location of internal defects. The capability of this test seemed to not be dependent on the location of weld gun and part contact. Results were most reliable when care was taken to not over-constrain the part, which is reflected in the final fixture design.

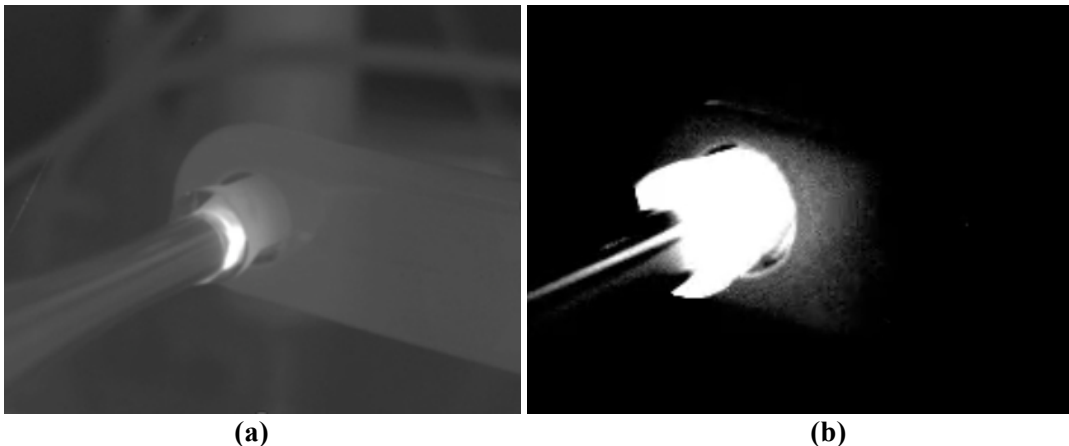


Figure 26. (a) Test showing the steel nub absorbing all the energy from the weld gun. The crank arm had no indication of heat change throughout the entirety of the test. Crank arm C3. (b) Crank arm with defect indicating no energy transfer into the crank arm. Crank arm F9731.

As shown in Figure 25, a previous test location was highlighted by a subsequent test, suggesting that some amount of damage was inflicted at or near the surface at the point of contact of the weld gun during the

previous test. There were also various levels of surface marring on the crank arms. We did not notice any change in the defect size due to multiple tests, so the destructive nature for the crank arms seems to be apparent only at the point of weld gun contact. Thus, we would recommend this test for finding the precise locations of defects during fatigue testing or other R&D practices. Even in these R&D scenarios, it would be good to mark where the contact points were from previous tests to ensure no defects are unaccounted for. We would not, however, recommend this test as it stands as a method to implement into a QA check on parts that customers will receive.

In an effort to avoid any contact between the weld gun and crank arm, we attempted to use a pedal spindle that was faced down to a nub for the contact point. As seen in Figure 26, the steel nub absorbed too much of the energy, and vibrated within the threads. Both of these caused heat signatures to appear in locations that were not defects. We were able to see similar effects when we attempted to vibrate the crank arm on the exposed aluminum surfaces. With these results, it seems that the most consistent way to reveal internal defects through vibrothermography is by using the weld gun on the carbon surface, which may result in surface marring.

VIII: Topics for Additional Research

This section briefly covers some potential areas to further build upon our research.

Originally Proposed Fixture

One topic worth consideration is to build the fixture that we originally designed and planned to be our final fixture design. This fixture features greater flexibility and versatility and may lend itself to a wider array of test specimen geometries. In addition, this fixture could be used to better optimize testing parameters and mounting for each specimen tested.

True NDT and Automation

Another opportunity for further improvement on our research is to investigate fully eliminating all damage done to the crank arms when tested, including surface marring. If this could be achieved, this test could plausibly be used as a QA check in the production environment for every crank arm that is produced. This would likely require the development of automating this process using machinery to load and unload crank arms and software to determine if the crank arm is defect-free.

Sine Sweep Thermography

One method that we found little reported research on is sine sweep thermography. In this method, rather than exciting the test piece with a set frequency of 20 kHz as in traditional vibrothermography, the test piece is subjected to a sweep of a range of frequencies. Per *The Influence of Excitation Frequency on the Effectiveness of Vibrothermographic Testing*, “It has been reported in the scientific literature that the narrowband frequency excitation is not an optimal choice for vibrothermographic measurements. The reason is that the measured thermal response on damage is influenced by the excitation frequency.” [13] This method may have benefits worth exploring if traditional vibrothermography gives unreliable results for other test specimens. Sweeping a range of frequencies may produce a good response from the test piece without requiring as much control over all other test variables (i.e. durometer of rubber pieces clamping test piece, torque to which the fastening bolts are tightened, pressure at interface of energy source and test piece, etc.). It is possible that a sine sweep could eliminate the need for all of these variables to be re-optimized for each new test specimen.

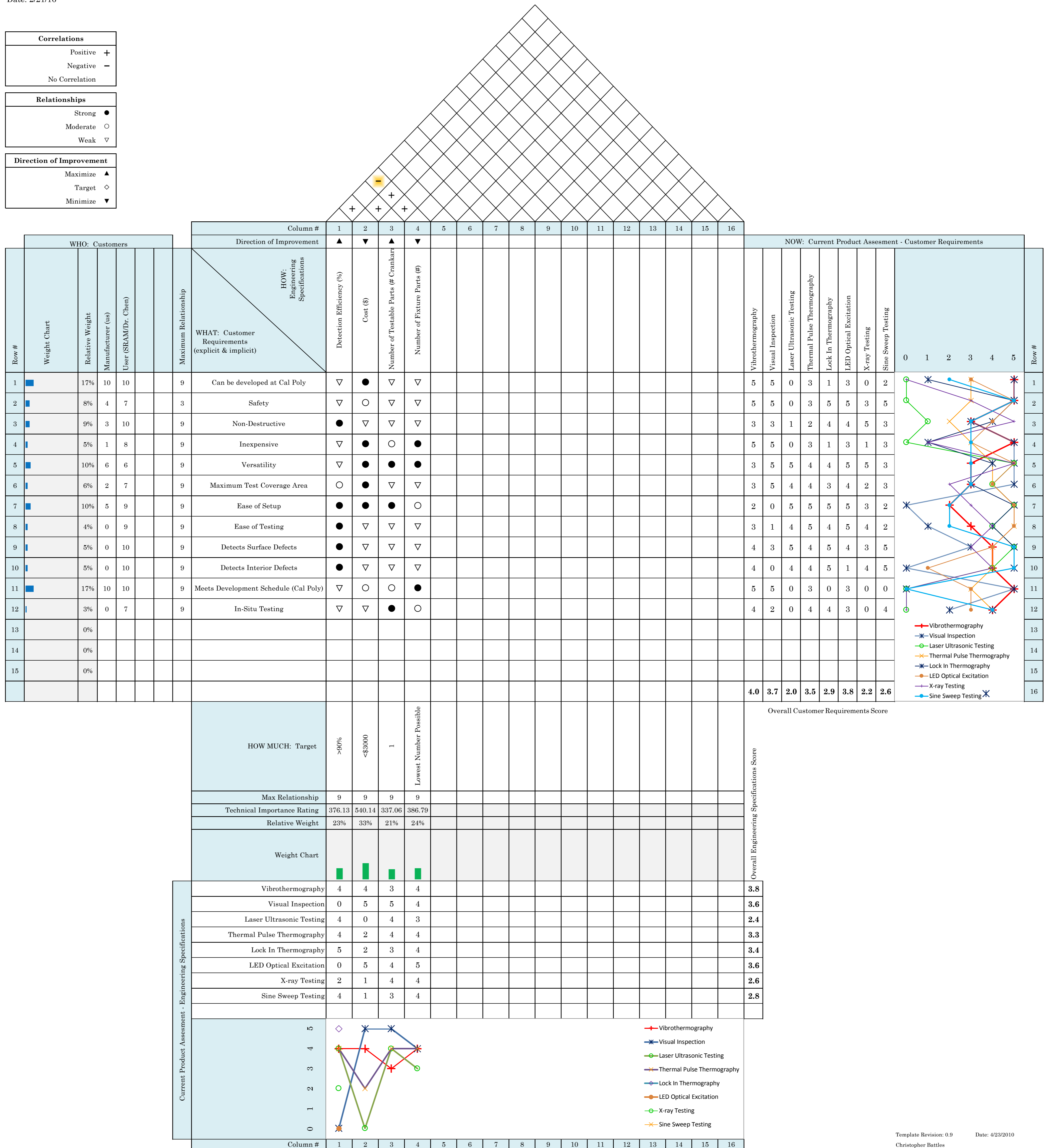
APPENDICES

QFD: House of Quality
 Project: NDT
 Revision: 2
 Date: 2/21/16

Correlations	
Positive	+
Negative	-
No Correlation	

Relationships	
Strong	●
Moderate	○
Weak	▽

Direction of Improvement	
Maximize	▲
Target	◇
Minimize	▼



APPENDIX C - DESIGN GOALS CONCEPT SELECTION MATRIX

Design Goals	Solutions		Clamp Solution					Mount Solution	Base Solution
			Line Contact Clamp Bars	Crank Hardware	Area/Contoured Contact	Top Bottom Edge Grip	V-block	Slot plate	Two uprights
Energy Transfer	Material at interface	<i>want to vary</i>	can vary	limited	can vary	can vary	can vary	-	-
	Type of contact (geometry)	<i>good or bad</i>	<i>unknown</i>	<i>unknown</i>	<i>unknown</i>	<i>unknown</i>	<i>unknown</i>	-	-
	Location of contact	<i>want to vary</i>	can vary	limited	limited	limited	can vary	can vary	can vary
Adjustability	Part slide	<i>possible?</i>	yes	no	no	maybe	yes	-	-
	Part flip	<i>possible?</i>	yes	no	no	yes	yes	-	-
	Mount slide	<i>possible?</i>	-	-	-	-	-	yes	-
	Mount flip	<i>possible?</i>	-	-	-	-	-	yes	-
	Base movement	<i>possible?</i>	-	-	-	-	-	-	yes
Visibility	Part adjustment	<i>possible?</i>	yes	no	no	yes	yes	-	-
	Clamp solution (blocking)	<i>good or bad</i>	okay	good	bad	good	okay	-	-
Repeatability	Limit orientations	<i>good or bad</i>	bad	good	good	bad	bad	bad	good
	Locating blocks	<i>possible?</i>	-	-	-	-	-	yes	-
	Number of fastened joints	<i>good or bad</i>	bad	good	bad	bad	bad	bad	good

Numerical Analysis

Design Goals	Solutions		Clamp Solution					Mount Solution	Base Solution
			Line Contact Clamp Bars	Crank Hardware	Area/Contoured Contact	Top Bottom Edge Grip	V-block	Slot plate	Two uprights
Energy Transfer	Material at interface	<i>want to vary</i>	1	0	1	1	1	-	-
	Type of contact (geometry)	<i>good or bad</i>	<i>unknown</i>	<i>unknown</i>	<i>unknown</i>	<i>unknown</i>	<i>unknown</i>	-	-
	Location of contact	<i>want to vary</i>	1	0	0	0	1	1	1
Adjustability	Part slide	<i>possible?</i>	1	0	0	1	1	-	-
	Part flip	<i>possible?</i>	1	0	0	0.5	1	-	-
	Mount slide	<i>possible?</i>	-	-	-	-	-	1	-
	Mount flip	<i>possible?</i>	-	-	-	-	-	1	-
	Base movement	<i>possible?</i>	-	-	-	-	-	-	1
Visibility	Part adjustment	<i>possible?</i>	1	0	0	1	1	-	-
	Clamp solution (blocking)	<i>good or bad</i>	0.5	1	0	1	0.5	-	-
Repeatability	Limit orientations	<i>good or bad</i>	0	1	1	0	0	0	1
	Locating blocks	<i>possible?</i>	-	-	-	-	-	1	-
	Number of fastened joints	<i>good or bad</i>	0	1	0	0	0	0	1
TOTAL			5.5	3	2	4.5	5.5	4	4

APPENDIX D - COST REPORT

Line	Product	Price	Unit	Qty	Extended Price	Vendor
1	1/4" End Mill	\$21.46	Ea	1	\$21.46	McMaster
2	1/2" End Mill	\$57.91	Ea	1	\$57.91	McMaster
3	40A Duro. 1/4" Rubber	\$25.49	Ea	1	\$25.49	McMaster
4	60A Duro. 1/4" Rubber	\$25.49	Ea	1	\$25.49	McMaster
5	JB Weld	\$17.50	Ea	1	\$17.50	McMaster
6	1/4-20 SS. Sock. Head Cap Screws	\$4.91	Pk-10	1	\$4.91	McMaster
7	Raw Aluminum 4 x 6 x 0.5	\$11.89	Ea	2	\$23.78	McMaster
8	Duct Tape	\$11.71	Ea	1	\$11.71	McMaster
9	Step Setup Clamps	\$9.15	Ea	2	\$18.30	McMaster
10	Clamp Adjustment Block	\$5.15	Ea	2	\$10.30	McMaster
Total					\$216.85	

Non-Destructive Carbon Fiber Crank Arm Test Plan

Introduction

Vibrothermography testing is going to be performed on the SRAM Force crank arm in order to find out if the crank arm's structure will allow the viewing of internal defects when excited by the weld gun at 20,000 Hz, as well as find out if the test can be accomplished without any form of damage to the crank arm itself. The test will be used in order to gain knowledge into finding the best settings and setup for future testing needs. This test will also be used to determine if the detection of defects is accurate and consistent.

Facilities and Apparatuses to be Utilized

- Utilizing the testing setup provided by Dr. John C. Chen at California Polytechnic State University, San Luis Obispo Building 192, room 102
- The facilities includes:
 - Air piston
 - Controlled by valves in order to control filling and removing air from the piston
 - Pressure measured with a Duro United pressure gauge that has an analog resolution of 0.2 PSI
 - Branson Weld Gun controlled by Branson 900M Weld Gun Controller
 - External trigger utilized to maintain safe distance away from weld gun tip
 - Compressed air
 - Computer to run the camera software that receives the raw image data from the camera
 - Fixture table
 - FLIR Indigo Phoenix infrared camera

Test Purpose

The purpose of this test is to determine if vibrothermography is a suitable non-destructive test method for the testing of carbon fiber crank arms. The results will be utilized by SRAM in order to evaluate their internal crank arm fatigue testing to find failure points without destroying crank arms.

Data to be Collected

The data that is to be collected is a collection of the best testing parameters that give the most consistent heat signatures as indicated by the infrared image sequences that are obtained through the camera and software. The data is to be analyzed in order to find out if the heat signature is indicative of a real defect or if the test produced a false positive.

Analysis to be Performed

At the time of testing, images from the camera software will be able to be analyzed immediately after the testing run has completed. This quick analysis will let us know if the testing parameter change increases or decreases the heat signature at locations with defects.

Once the testing has been completed, the TIF files will be analyzed through image processing utilizing the software “imageJ” to change the color scale of the image. The raw data is in the format of grayscale, making the image difficult to analyze, in order to change this, the dynamic range of the image is adjusted to make the scale brighter, that is, the lightest gray becomes white and the darkest gray because black. In order to make the defects more apparent, the resting state is subtracted from each pixel, leaving the user with the difference in temperatures from steady state to the final heating state, which is what is desired to find the heat signatures at the defect locations.

Part and Setup Changes

Between every one or two tests, the tape used as the interfacing material between the gun and the part will need to be interchanged. This will require removal of the crank arm, removal of the tape, replacement of the tape, and remounting of the crank arm. When this is done, the gun placement might change by a miniscule amount. The reason for replacing the tape is to ensure the surface of the crank arm isn’t damaged.

In order to completely test each parameter, different magnitudes of each factor must be checked utilizing the OFAT (one factor at a time) testing method. The parameters will be tested in the order provided:

1. Total energy input as controlled by the weld gun controller.
2. Pressure behind weld gun measured as the pressure in the air cylinder pressing the weld gun tip against the crank arm test piece. This value is measured in PSI.
3. Clamping configuration is controlled by the user and which method they have clamped, either one front plate on either side, both front plates, no back plates, or mounted by the bottom bracket lug.
4. Gun placement is controlled by the user, and determines what the backing surface is behind the carbon fiber layers.
5. Coupling method is determined by which type of tape is used to separate the weld gun tip from the surface of the carbon fiber, as well as increase the coupling of the system which allows more energy input to the system.
6. Rubber durometer determines how heavily the crank arm damps the mechanical excitement during testing.

Multiple crank arms will be tested, thus requiring the setup to be completed again.

Test Procedure

1. Start the computer
2. Set up the infrared camera
3. Open the software that allows for focusing of the camera and proceed to focus the camera
4. Turn weld controller on and set time and energy output levels to desired values
5. Ensure upright is rigidly attached to the table
6. Clamp back plates onto uprights
7. Prepare crank arm with the correct coupling interface material
8. Place part in position desired
9. With the pressure turned on, open the valve for the air piston inlet until the indicated pressure is the desired value.
 - a. This will also hold the test piece in place if there are no front plates being used.
10. With the camera field of view clear of any external heat sources, adjust the camera to set the colors of the output image, making the coldest areas dark and warmest areas white, with a gradient between the high and low values.
11. Click “Acquire” on the software, which will capture the next set number of images and store them locally in a cache until saved.
12. Press the external switch in order to “fire” the weld gun, which will excite the test piece.
13. Observe heat signatures from part excitation
14. Save files as both .TIF and the raw native data file for the software.

Test Results

Data Table

Test #	Energy Input	Pressure Behind Gun	Clamp Method	Gun Placement	Coupling Method	Rubber Durometer	Notes
	[Joules]	[PSI]	[Description]	[Description]	[Interface Material]	[Hardness]	[Description]
1							
2							
3							
4							
5							

Note of Failures

Any failures should be noted, including the cause in order to ensure that no failure occurs again. The following form should also be completed if any failures occurred.

Failed Part Name:	
Time of Failure:	
Operator:	
Cause of Failure:	
Notes:	
Picture(s):	

Conclusions and Recommendations

Utilizing the data obtained, conclusions from the testing should be drawn and noted. Future testing recommendations should also be noted in order to improve future testing sessions, and fix anything that may have gone wrong during testing.

What Worked Well:	
What Worked Poorly:	
Suggestions:	

Non-Destructive Testing Manufacturing Plan

Parts Not Requiring Manufacturing

- All crank arms being tested
 - SRAM Force Crank Arm, GXP Bottom Bracket Lug
 - SRAM Red Crank Arm, BB30 Bottom Bracket Lug
- Fixture table
 - Provided by lab facilities under Dr. John C. Chen at California Polytechnic State University, San Luis Obispo Building 192 Room 102
- Upright for preliminary testing
 - Provided in lab
- Hardware
 - Most of the Stainless hardware used was had on hand in the lab
- Weld Gun
 - Provided in lab

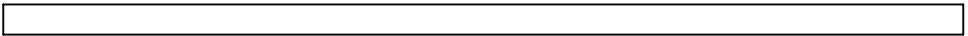
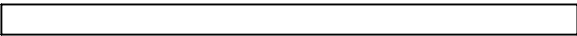
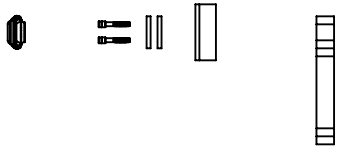
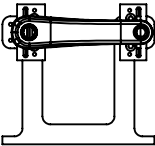
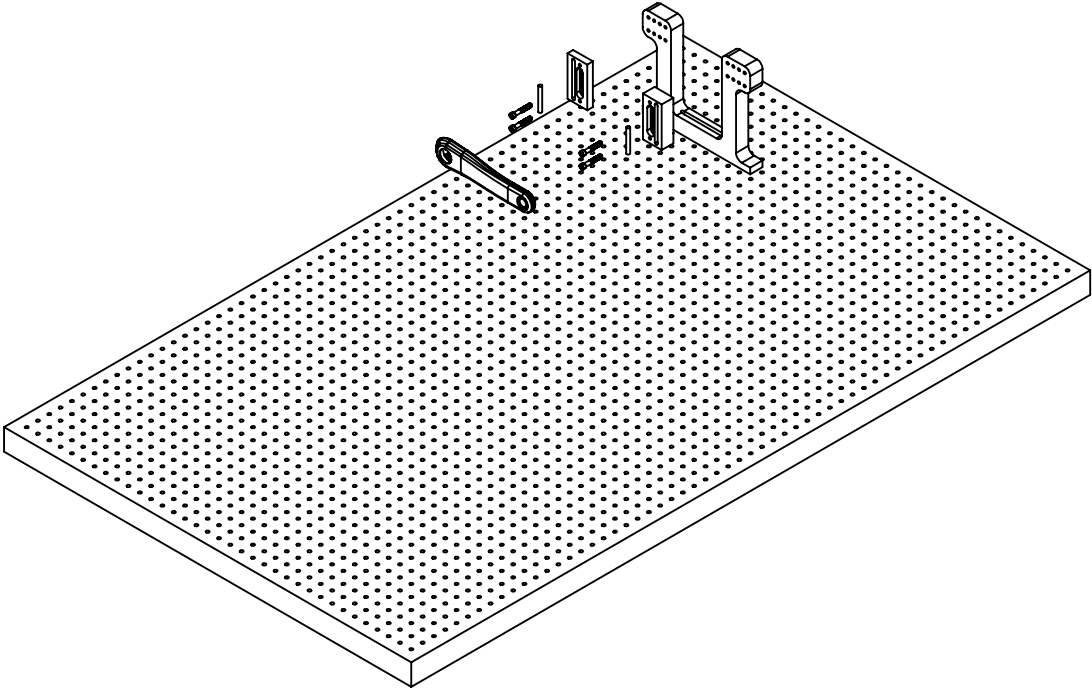
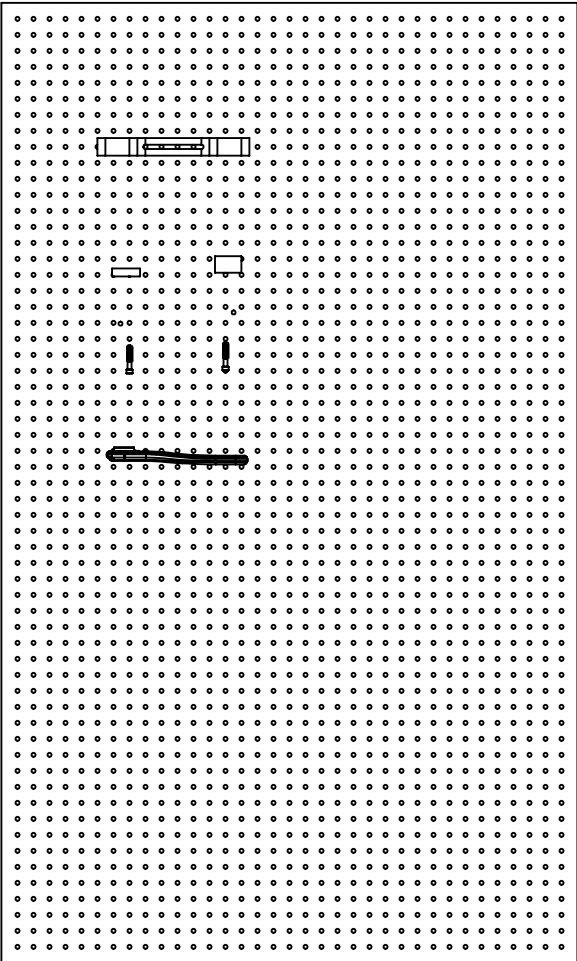
Parts Requiring Manufacturing

- Left and Right Mounts (1X each)
 - To be done on a manual mill
 - ¼” and ½” tooling for through slots
 - ¼” ball end mill for rubber carrier slot
 - #7 drill bit used as pilot holes for the ¼” - 20 tap
 - Raw material had on hand
 - Estimated machining time (including cleanup): 180 minutes for both mounts
- Outer Mount (2X)
 - To be done on a manual mill
 - ¼” ball for rubber carrier slots
 - Size H drill bit used for clearance holes
 - Estimated machining time (including cleanup): 90 minutes for both pieces
- Spindle mount plate
 - Material: ¼” carbon steel (on hand)
 - Plasma cut rough dimensions
 - Machine outsides and hole pattern on vertical mill
 - Surface prep for welding on of GXP spindle
- Spindle (GXP)
 - Cut spindle off of drive side crank arm
 - Face to length on manual lathe
 - Prep surface area which will be welded to spindle mount plate
 - Fillet weld with GTAW (TIG) welding to plate

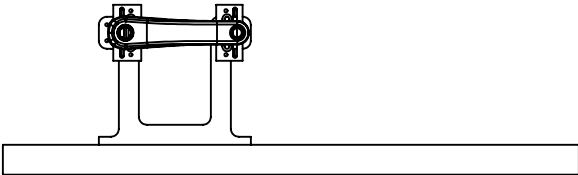
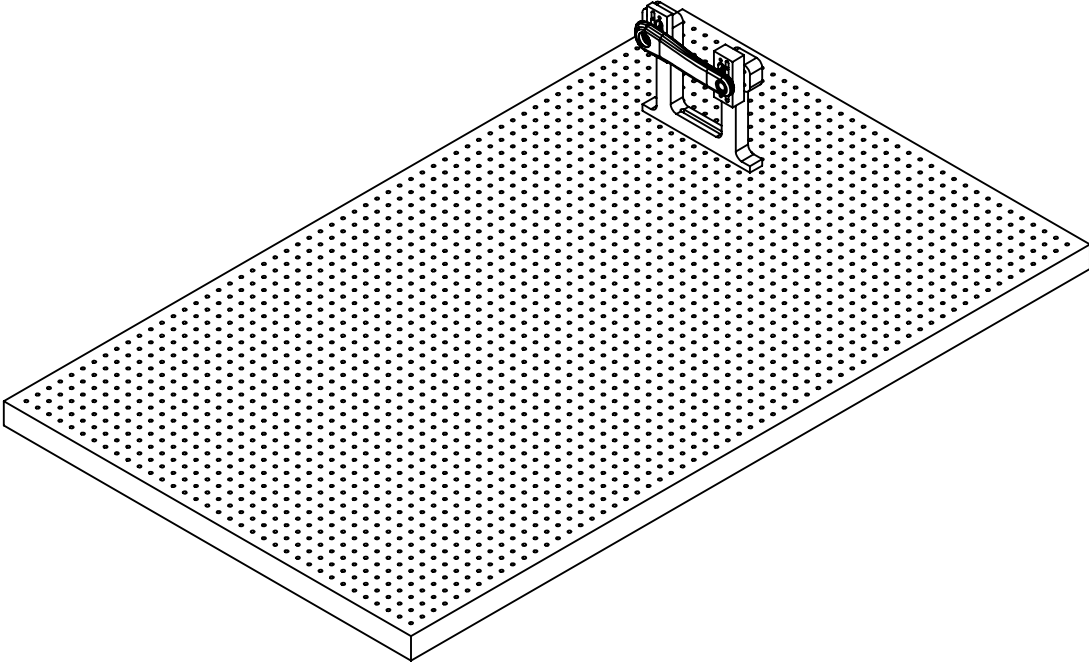
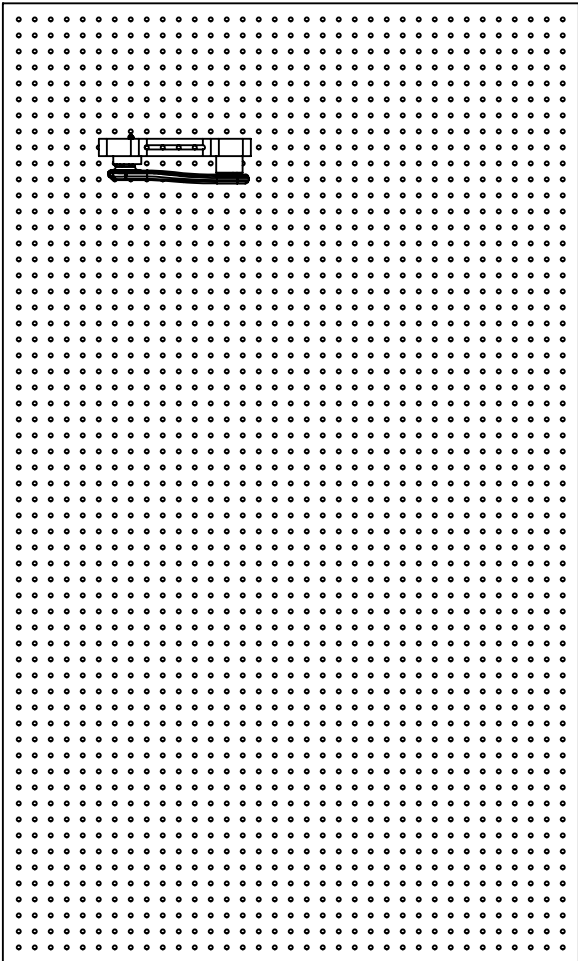
- Spindle (GXP)
 - Cut spindle off of drive side crank arm
 - Face to length on manual lathe
 - Prep surface area which will be welded to spindle mount plate
 - Fillet weld with GTAW (TIG) welding to plate

APPENDIX G - DFMEA

Item / Function	Potential Failure Mode	Potential Effect(s) of Failure	Sev	Potential Cause(s) / Mechanism(s) of Failure	Occur	Crit	Recommended Action(s)	Responsibility & Target Completion Date	Action Results			
									Actions Taken	Sev	Occur	Crit
Upright	Slipping	Test Piece comes loose	5	Inadequate torque applied to fixturing hardware	1	5	Ensure proper torque on fixture hardware	Grant - 4/26/2016	Procedural requirement written into test plan	5	1	5
Upright	Slipping at table attachment	Gun slides across part	6	Inadequate torque applied to fixturing hardware	1	6	Ensure proper torque on fixture hardware	Grant - 4/26/2016	Procedural requirement written into test plan	6	1	6
Gun Tip	Minor Slipping	Destructive to the surface of the crank arm (if tested on resin surface)	3	Inadequate coupling method	2	6	Ensure tape application to test piece to reduce gun tip slipping	Grant - 4/26/2016	Procedural requirement	3	2	6
Crank Arm	Heat Saturation	Ineffective test with uncertain results	2	Not enough cool down time between tests	3	6	Pause between each subsequent test on each part until the piece has cooled to near room temperature	Johnathan - 5/3/2016	Procedural requirement	2	3	6
Crank Arm	Heat Saturation	Ineffective test with uncertain results	2	Not enough cool down time between tests	3	6	Pause between each subsequent test on each part until the piece has cooled to near room temperature	Johnathan - 5/3/2016	Procedural requirement	2	3	6

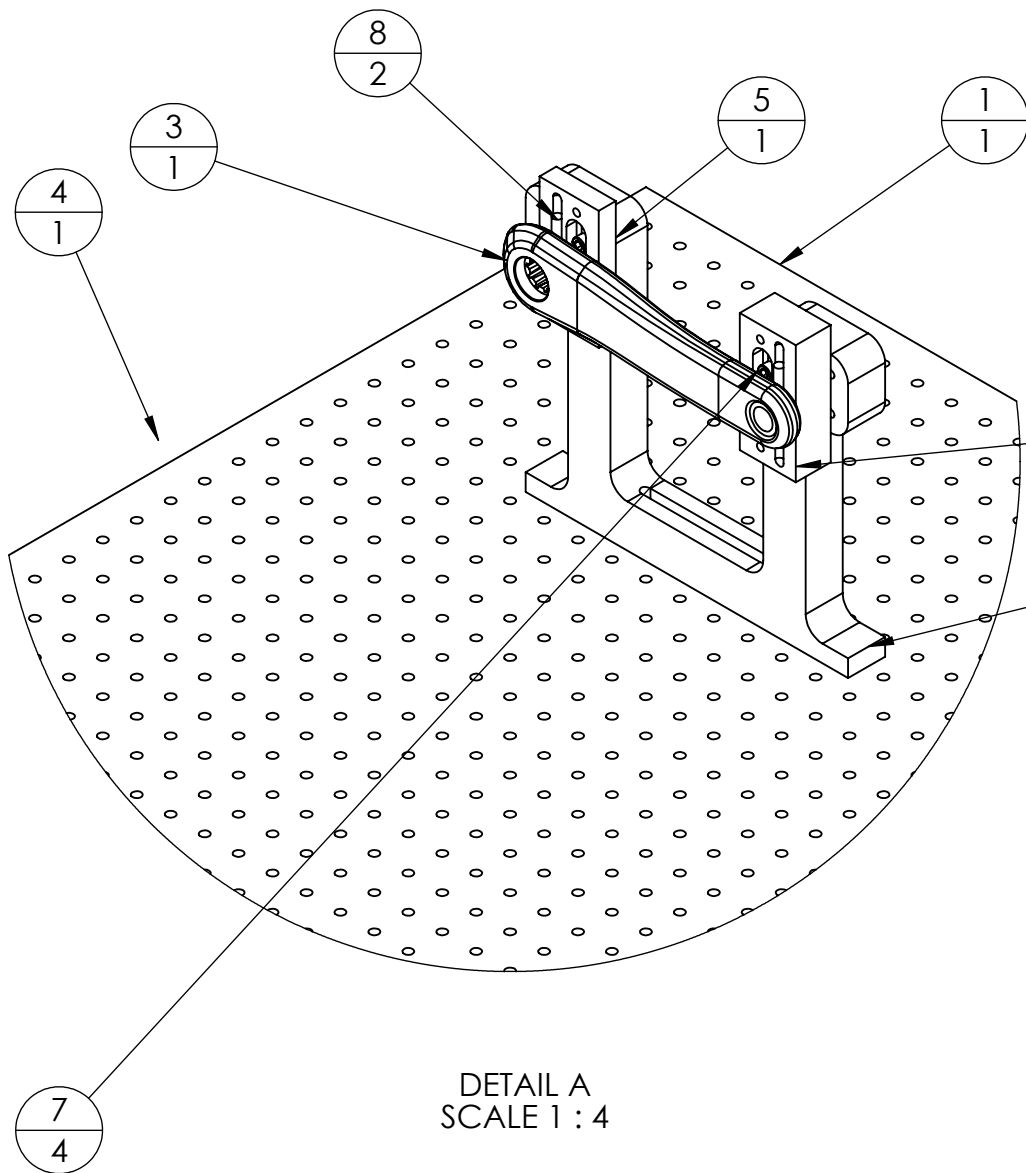


Cal Poly Mechanical Engineering	Tolerance: N/A	Material: N/A	Title: ASSEMBLY, TEST FIXTURE 2.2		Drwn. By: GRANT POCKLINGTON
	Dwg. #: A001-1	Asb: A001	Date: 4/30/2016	Scale: 1:12	Chkd. By: JOHNATHAN SIMEROTH

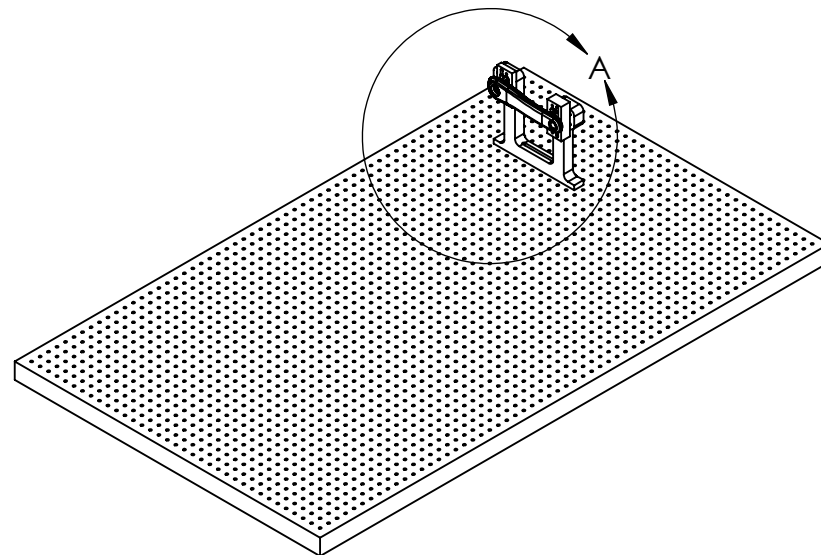


Cal Poly Mechanical Engineering	Tolerance: N/A	Material: N/A	Title: ASSEMBLY, TEST FIXTURE 2.2	Drwn. By: GRANT POCKLINGTON
	Dwg. #: A001-2	Asb: A001	Date: 4/30/2016	Scale: 1:12

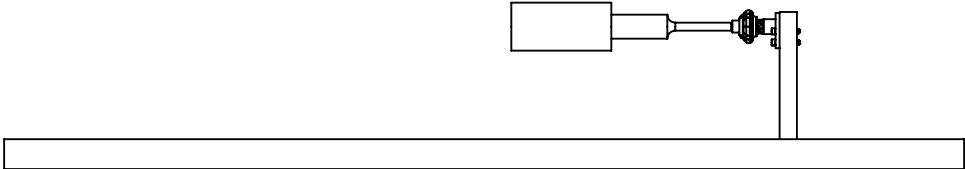
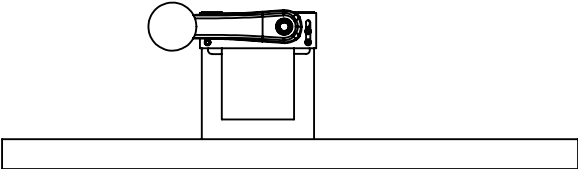
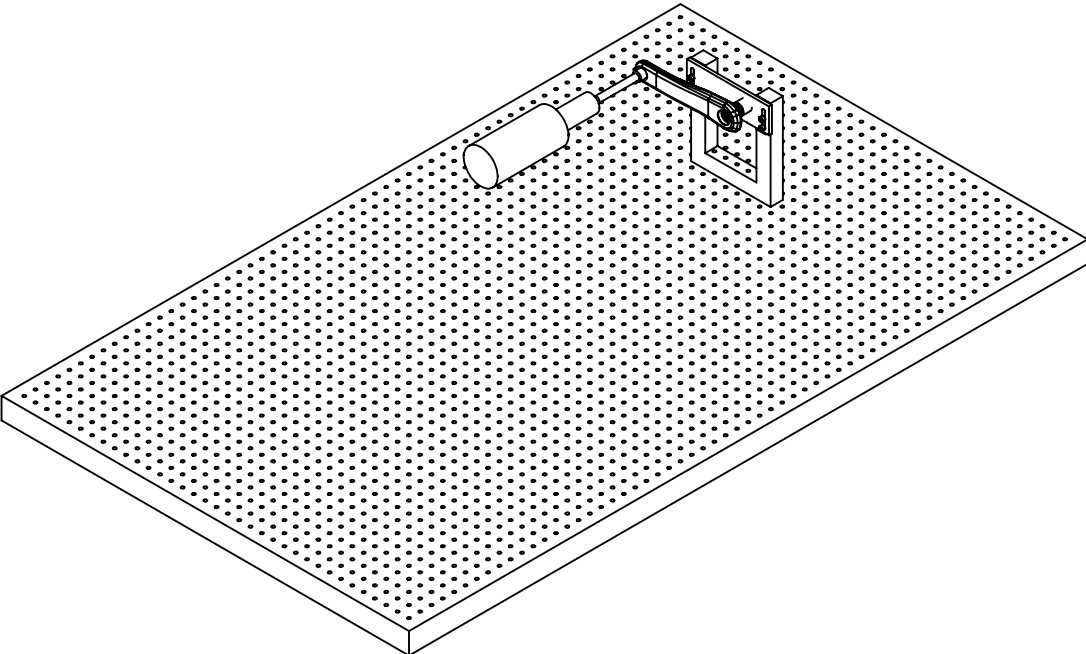
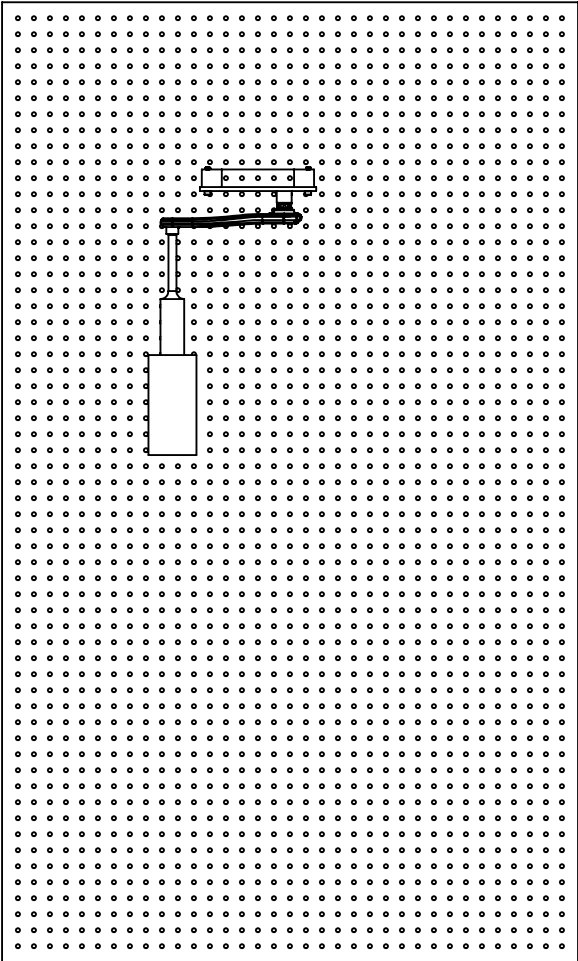
ITEM NO.	PART NUMBER	QTY.
1	TABLE	1
2	UPRIGHT REV 2	1
3	SRAM Force Crank Arm	1
4	WELD GUN	1
5	CBORED LEFT MOUNT REV 2	1
6	CBORED RIGHT MOUNT REV 2	1
7	92185A546	4
8	RUBBER BACK	2



DETAIL A
SCALE 1 : 4

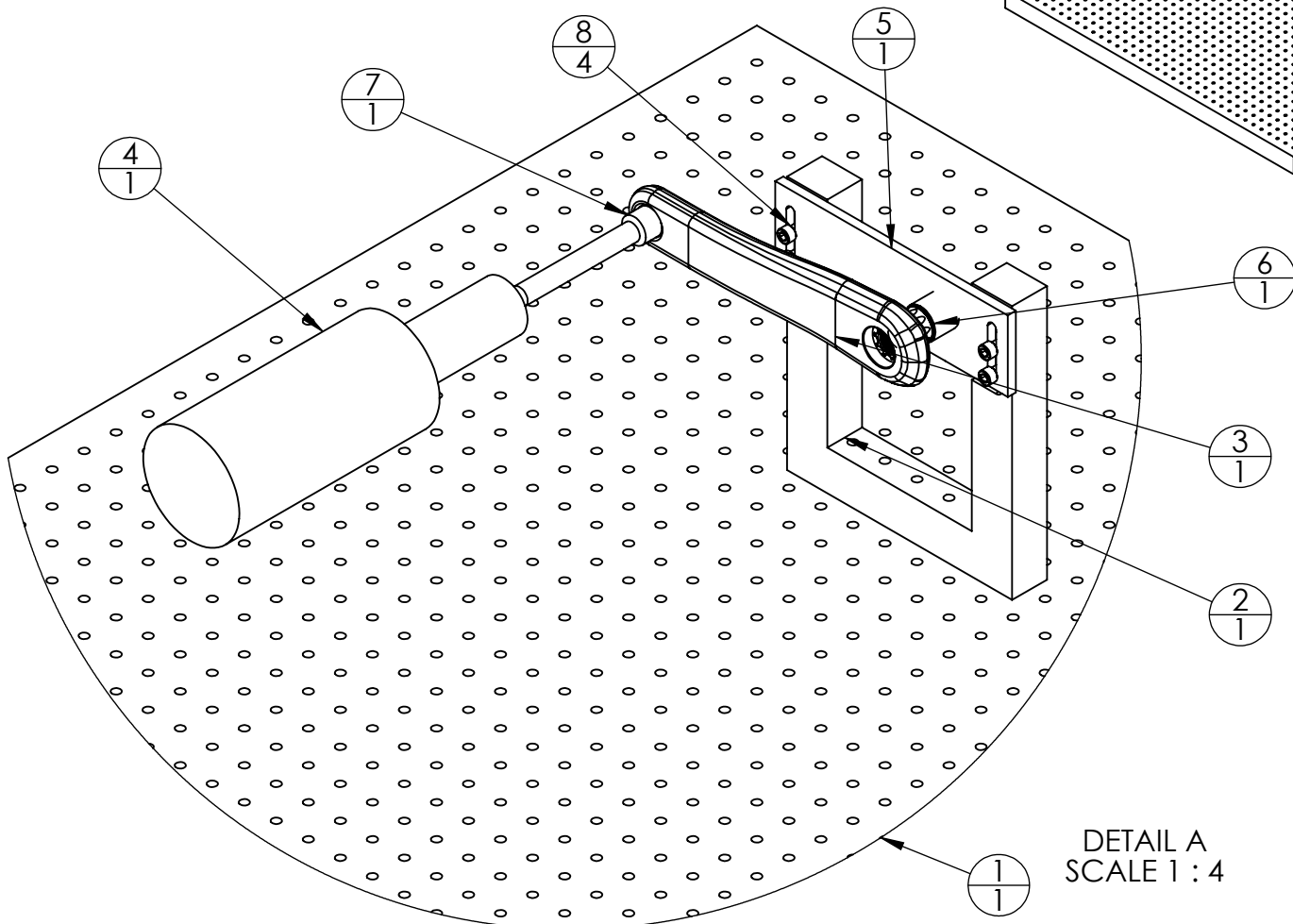
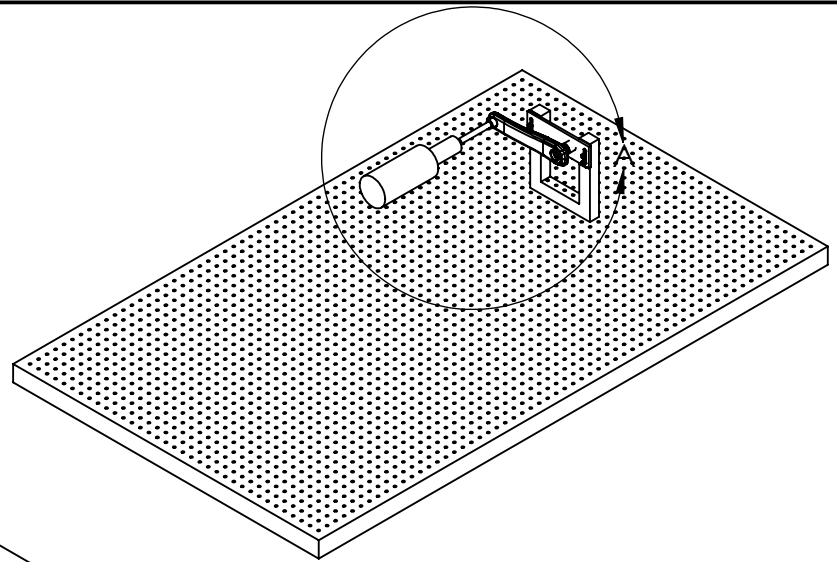


Cal Poly Mechanical Engineering	Tolerance: N/A	Material: N/A	Title: ASSEMBLY, TEST FIXTURE 2.2	Drwn. By: GRANT POCKLINGTON
	Dwg. #: A001-3	Asb: A001	Date: 4/30/2016	Scale: 1:16
				Chkd. By: JOHNATHAN SIMEROTH




Cal Poly Mechanical Engineering	Tolerance: N/A	Material: N/A	Title: ASSEMBLY, TEST FIXTURE 2.3		Drwn. By: GRANT POCKLINGTON
	Dwg. #: A002-1	Asb: A002	Date: 5/30/2016	Scale: 1:12	Chkd. By: JOHNATHAN SIMEROTH

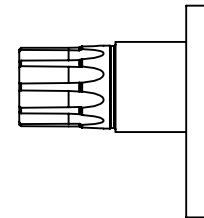
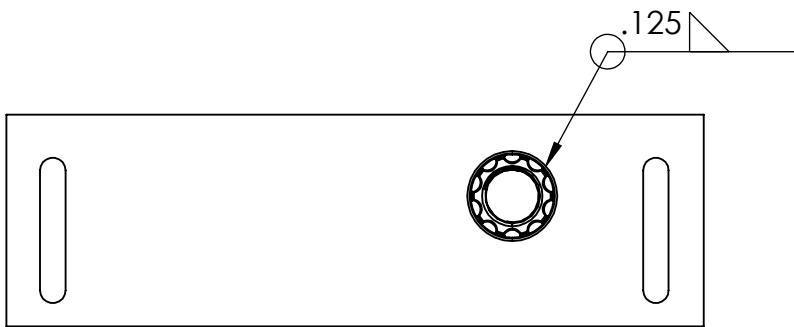
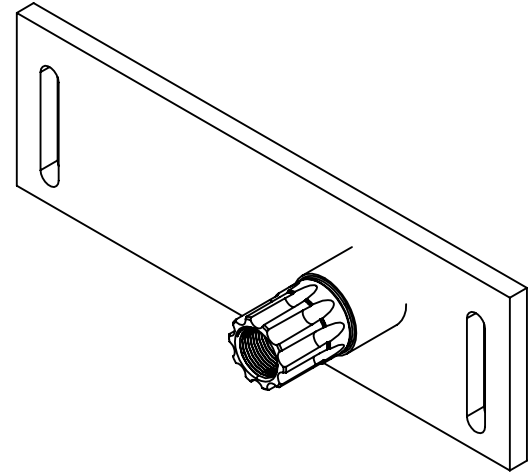
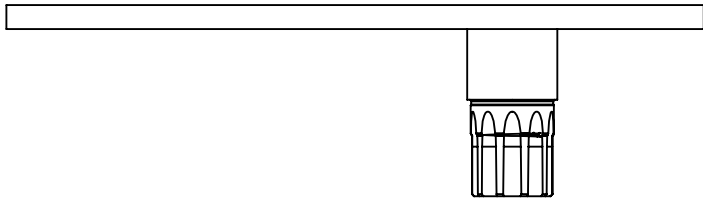
ITEM NO.	PART NUMBER	QTY.
1	TABLE	1
2	CHEN UPRIGHT	1
3	SRAM FORCE CRANK ARM	1
4	WELD GUN	1
5	SPINDLE BACKING PLATE	1
6	GXP SPINDLE	1
7	PEDAL GUN RECEIVER	1
8	92185A546	4



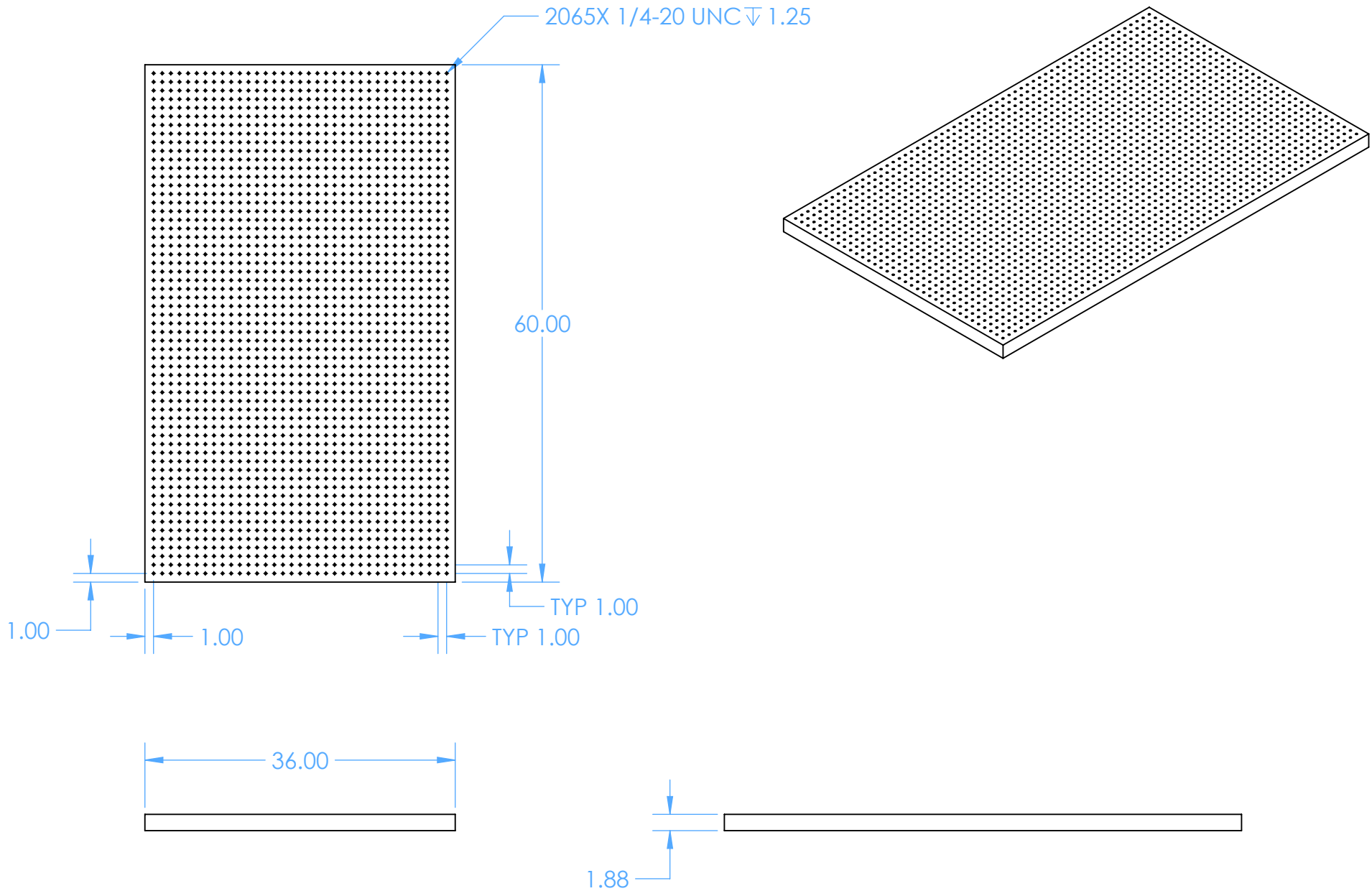
DETAIL A
SCALE 1 : 4

Cal Poly Mechanical Engineering	Tolerance: N/A	Material: N/A	Title: ASSEMBLY, TEST FIXTURE 2.3	Drwn. By: GRANT POCKLINGTON
	Dwg. #: A002-2	Asb: A002	Date: 5/30/2016	Scale: 1:12
				Chkd. By: JOHNATHAN SIMEROTH

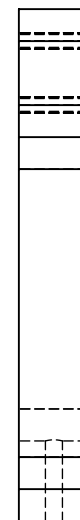
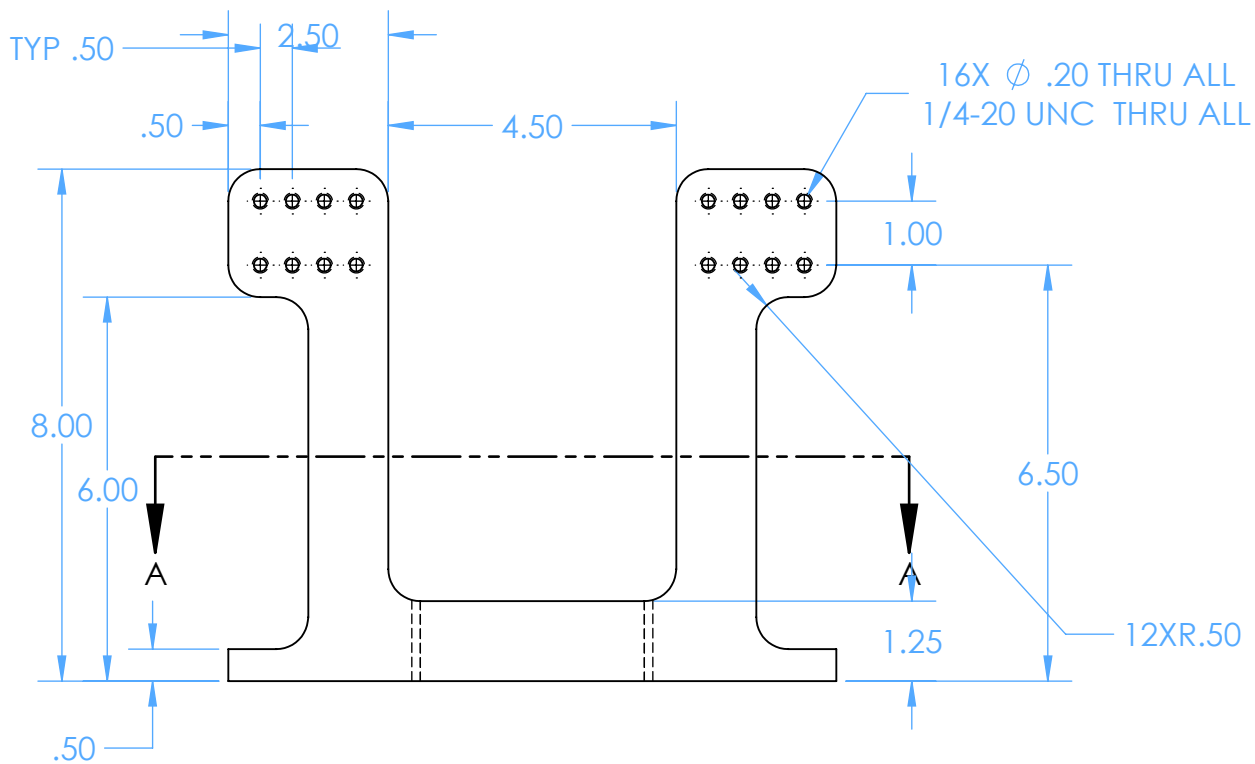
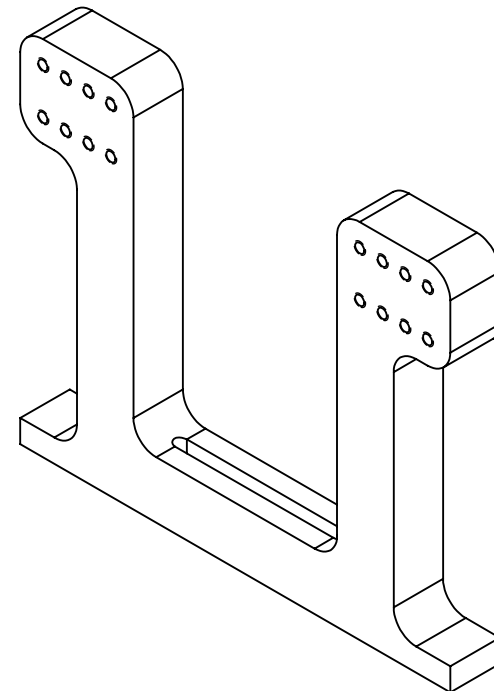
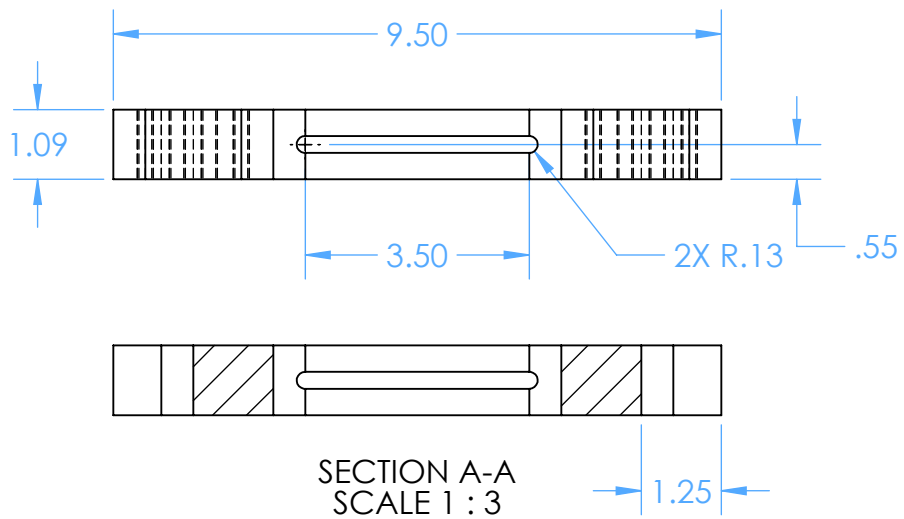
ITEM NO.	WELD SIZE	SYMBOL	WELD LENGTH	WELD MATERIAL	QTY.
1	.125		2.94	STEEL	1



Cal Poly Mechanical Engineering	Tolerance: N/A	Material: STEEL	Title: WELDMENT BB SPINDLE MOUNT	Drwn. By: GRANT POCKLINGTON
	Dwg. #: A002-4	Asb: A002	Date: 5/30/2016	Scale: 1:2
				Chkd. By: JOHNATHAN SIMEROTH



Cal Poly Mechanical Engineering	Tolerance: N/A	Material: ALU	Title: TABLE		Drwn. By: GRANT POCKLINGTON
	Dwg. #: P001	Nxt Asb: A001/A002	Date: 4/30/2016	Scale: 1:16	Chkd. By: JOHNATHAN SIMEROTH



Cal Poly Mechanical Engineering

Tolerance: $\pm .010$

Material: SST

Title: UPRIGHT

Drwn. By: GRANT POCKLINGTON

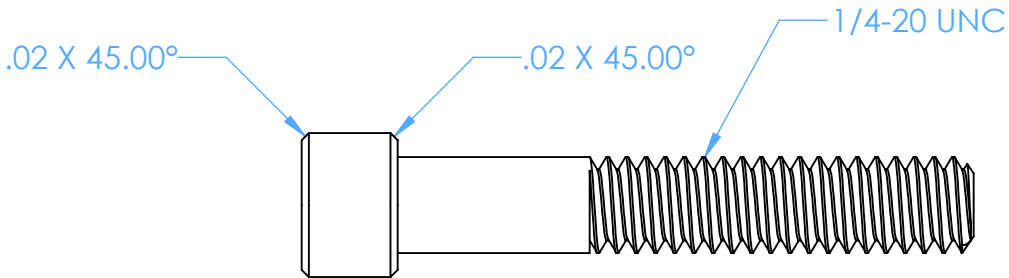
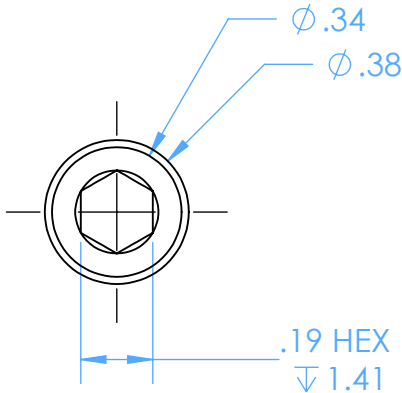
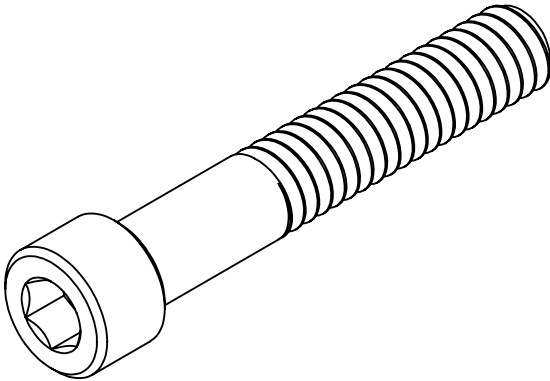
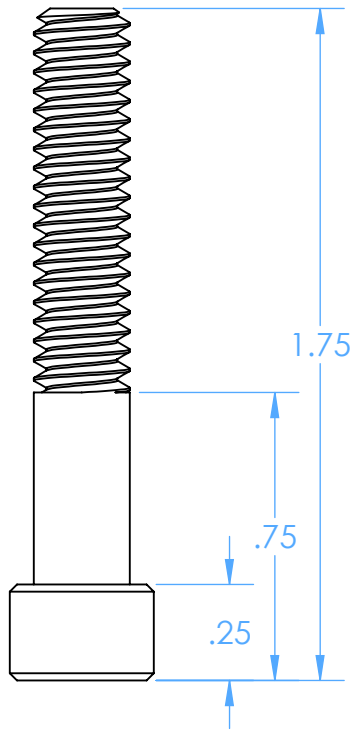
Dwg. #: P002

Nxt Asb: A001

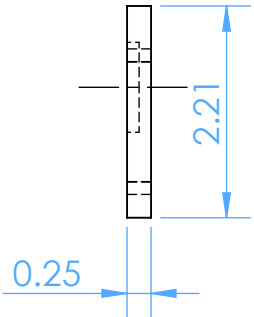
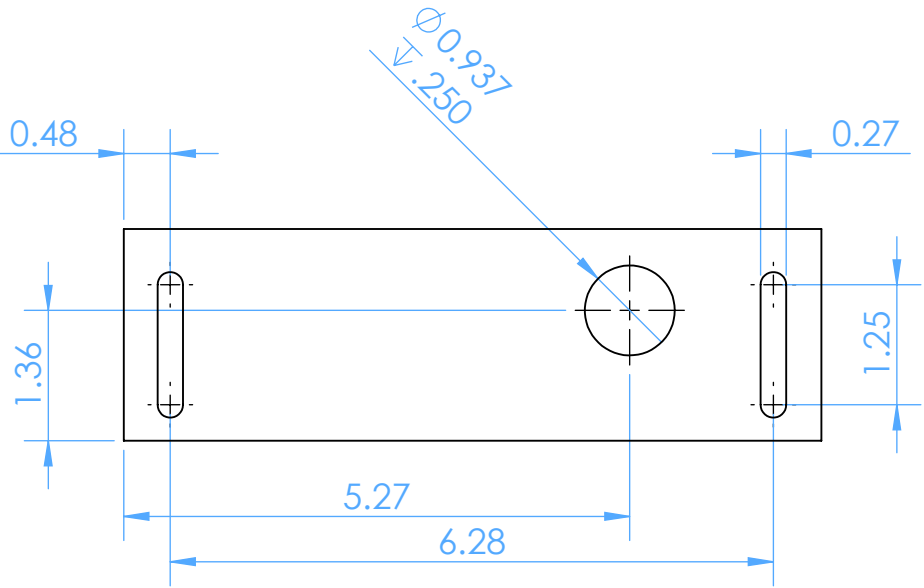
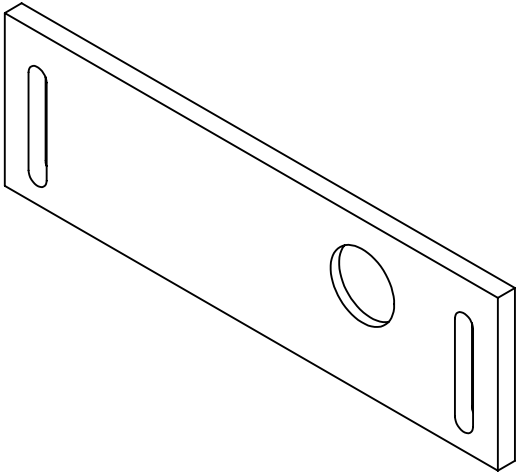
Date: 4/30/2016

Scale: 1:3

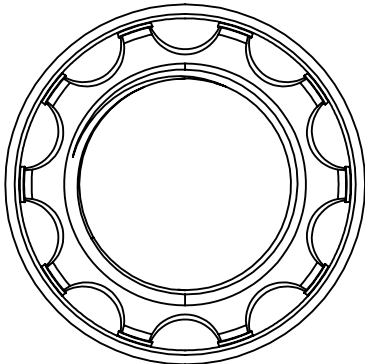
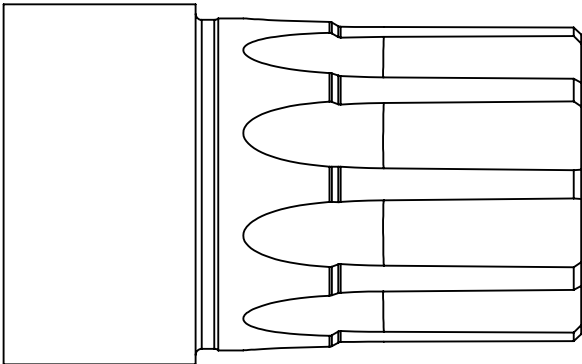
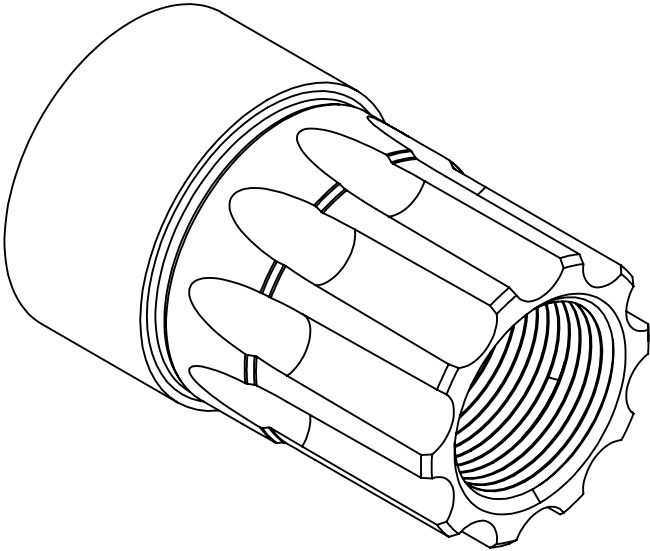
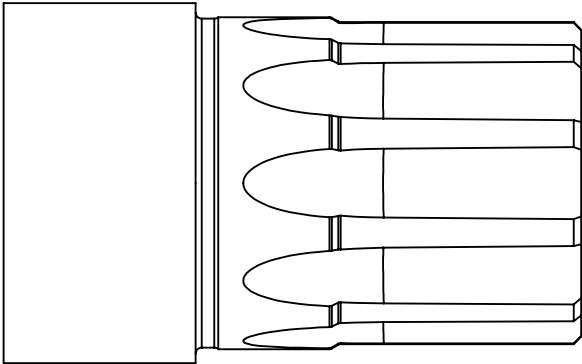
Chkd. By: JOHNATHAN SIMEROTH



Cal Poly Mechanical Engineering	Tolerance: N/A	Material: SST	Title: SCREWS MCM PART # 92185A546		Drwn. By: GRANT POCKLINGTON
	Dwg. #: P003	Nxt Asb: A001/A002	Date: 4/30/2016	Scale: 2:1	Chkd. By: JOHNATHAN SIMEROTH

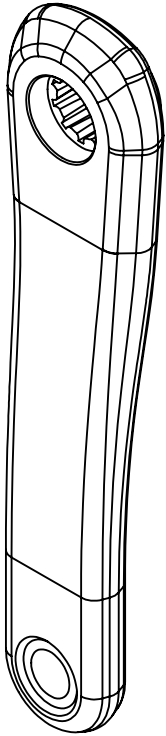
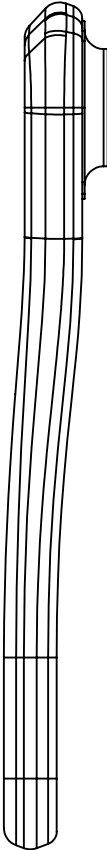
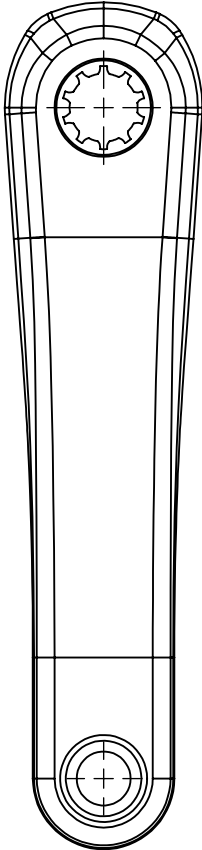
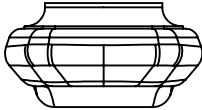


Cal Poly Mechanical Engineering	Tolerance: $\pm .01$	Material: STEEL	Title: SPINDLE BACKING PLATE		Drwn. By: GRANT POCKLINGTON
	Dwg. #: P004	Nxt Asb: A002	Date: 5/30/2016	Scale: 1:12	Chkd. By: JOHNATHAN SIMEROTH



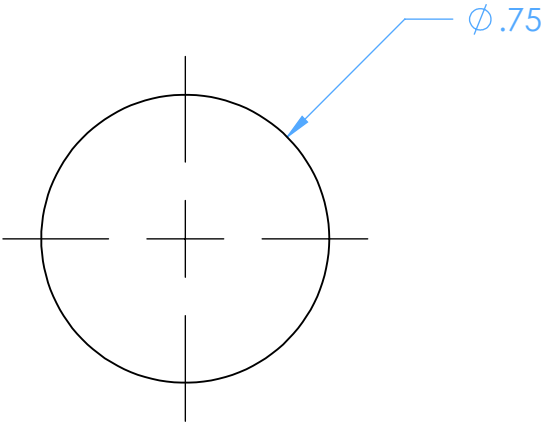
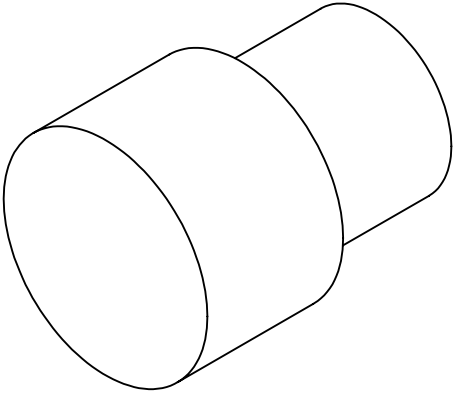
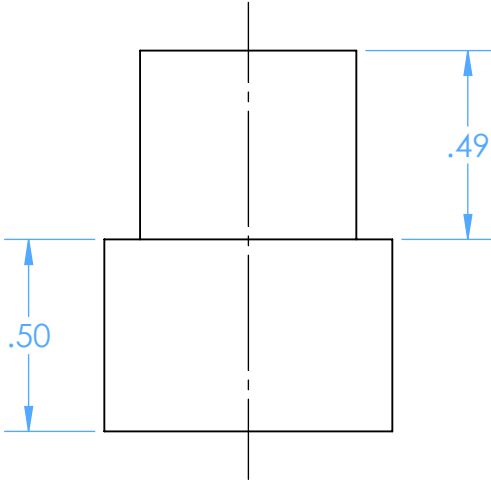
NOTE:
MODEL PROVIDED BY SRAM
DIMENSIONS WITHHELD

Cal Poly Mechanical Engineering	Tolerance: $\pm .01$	Material: STEEL	Title: GXP BOTTOM BRACKET SPINDLE		Drwn. By: GRANT POCKLINGTON
	Dwg. #: P005	Nxt Asb: A002	Date: 4/30/2016	Scale: 2:1	Chkd. By: JOHNATHAN SIMEROTH

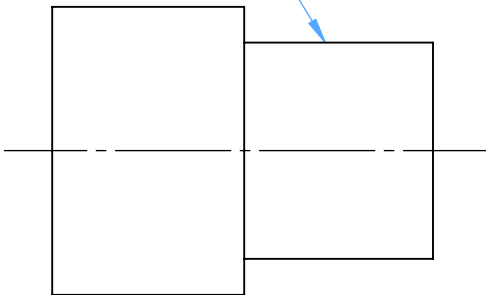


NOTE:
MODEL PROVIDED BY SRAM
DIMENSIONS WITHHELD

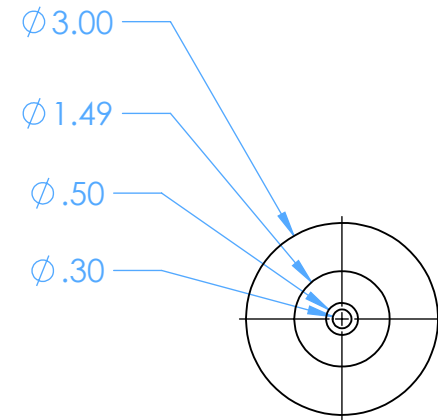
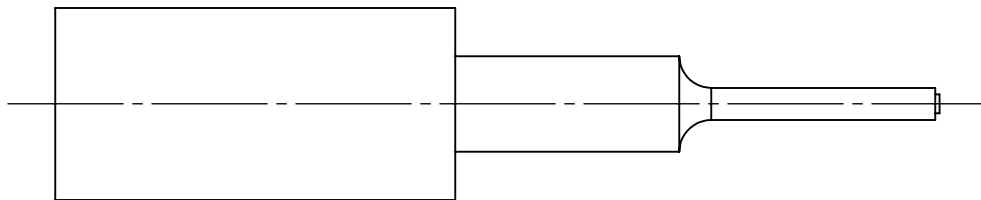
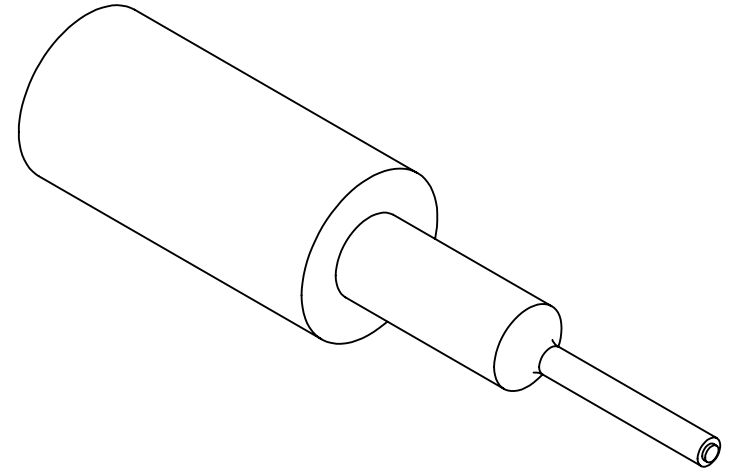
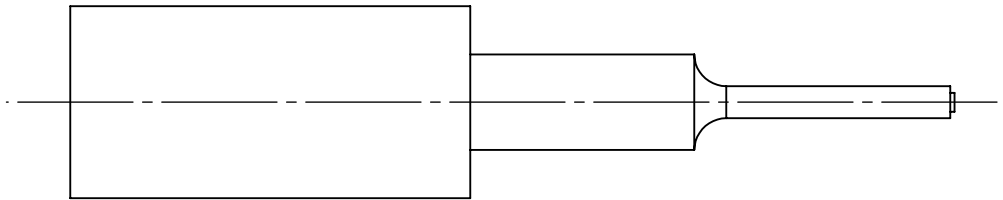
Cal Poly Mechanical Engineering	Tolerance: N/A	Material: CF	Title: SRAM FORCE CRANK ARM		Drwn. By: GRANT POCKLINGTON
	Dwg. #: P006	Nxt Asb: A001/A002	Date: 4/30/2016	Scale: 1:2	Chkd. By: JOHNATHAN SIMEROTH



9/16-20 THREADED
SPECIAL THREAD SIZE

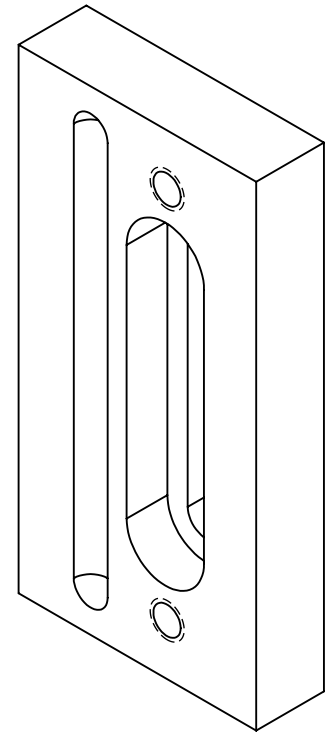
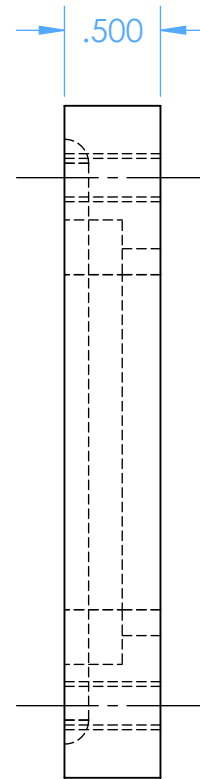
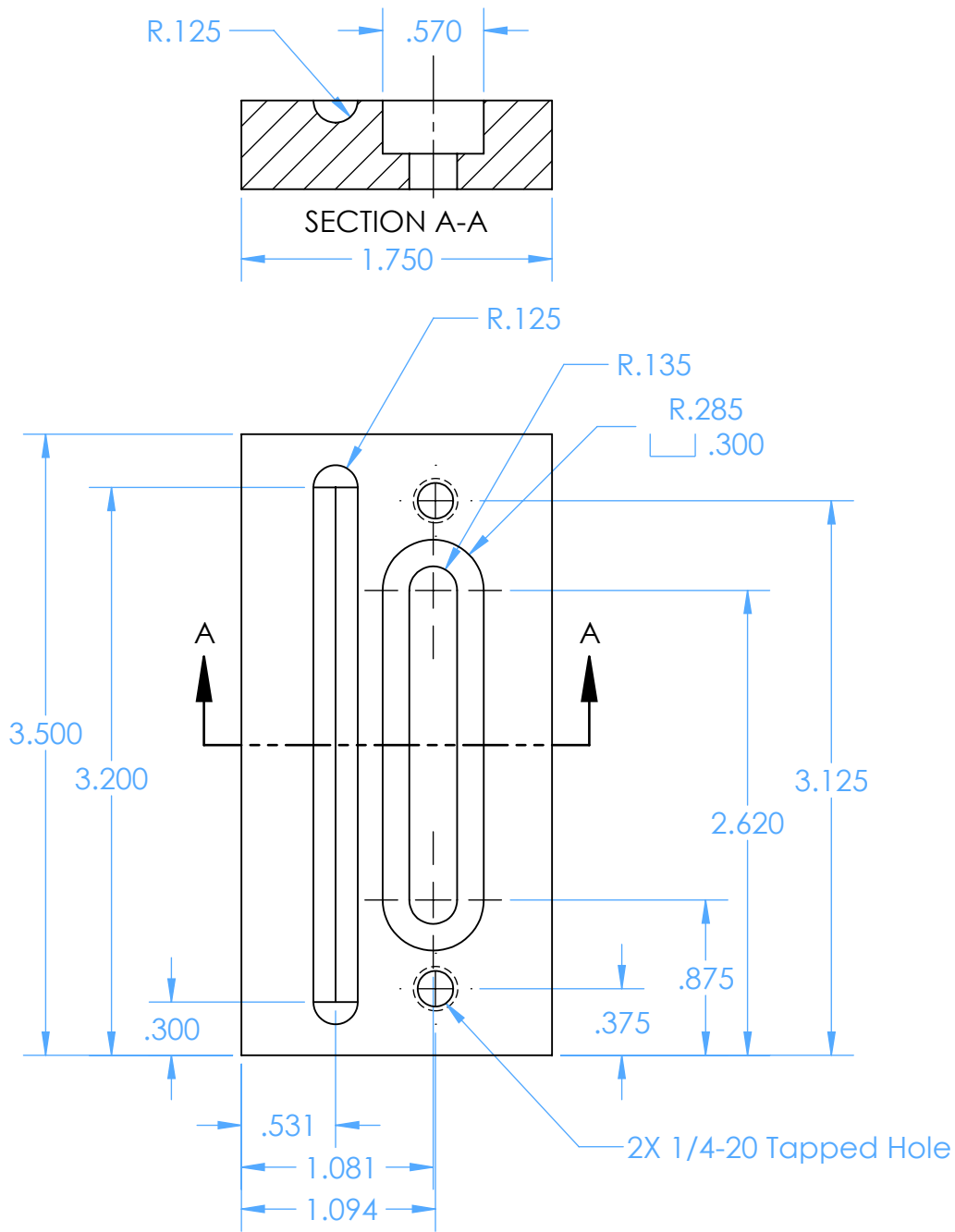


Cal Poly Mechanical Engineering	Tolerance: $\pm .01$	MATERIAL: ALU	Title: PEDAL SPINDLE GUN RECEIVER	Drwn. By: GRANT POCKLINGTON
	Dwg. #: P007	Nxt Asb: A002	Date: 4/30/2016	Scale: 2:1



MODEL REFERENCE, DIMENSIONS ARE ROUGH

Cal Poly Mechanical Engineering	Tolerance: N/A	Material: N/A	Title: WELD GUN		Drwn. By: GRANT POCKLINGTON
	Dwg. #: P008	Nxt Asb: A001/A002	Date: 4/30/2016	Scale: 1:3	Chkd. By: JOHNATHAN SIMEROTH



Cal Poly Mechanical Engineering

Tolerance: $\pm .005$

Material: ALU

Title: LEFT MOUNT

Drwn. By: GRANT POCKLINGTON

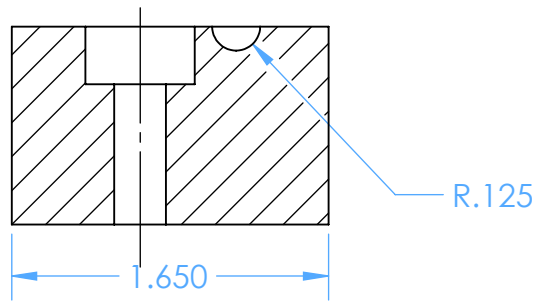
Dwg. #: P009

Nxt Asb: A001

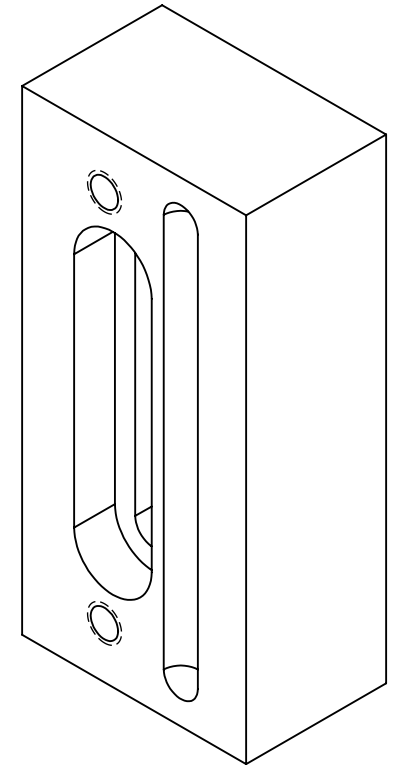
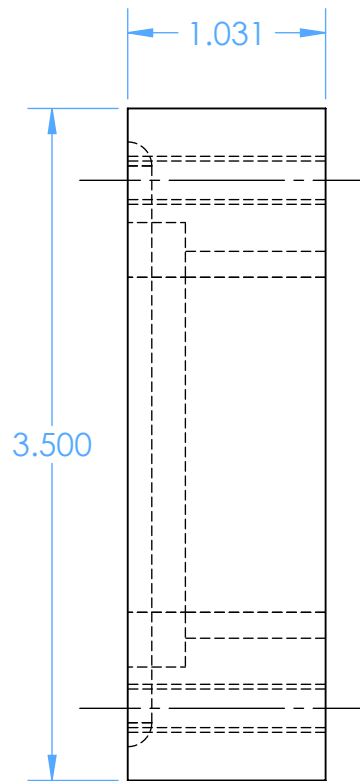
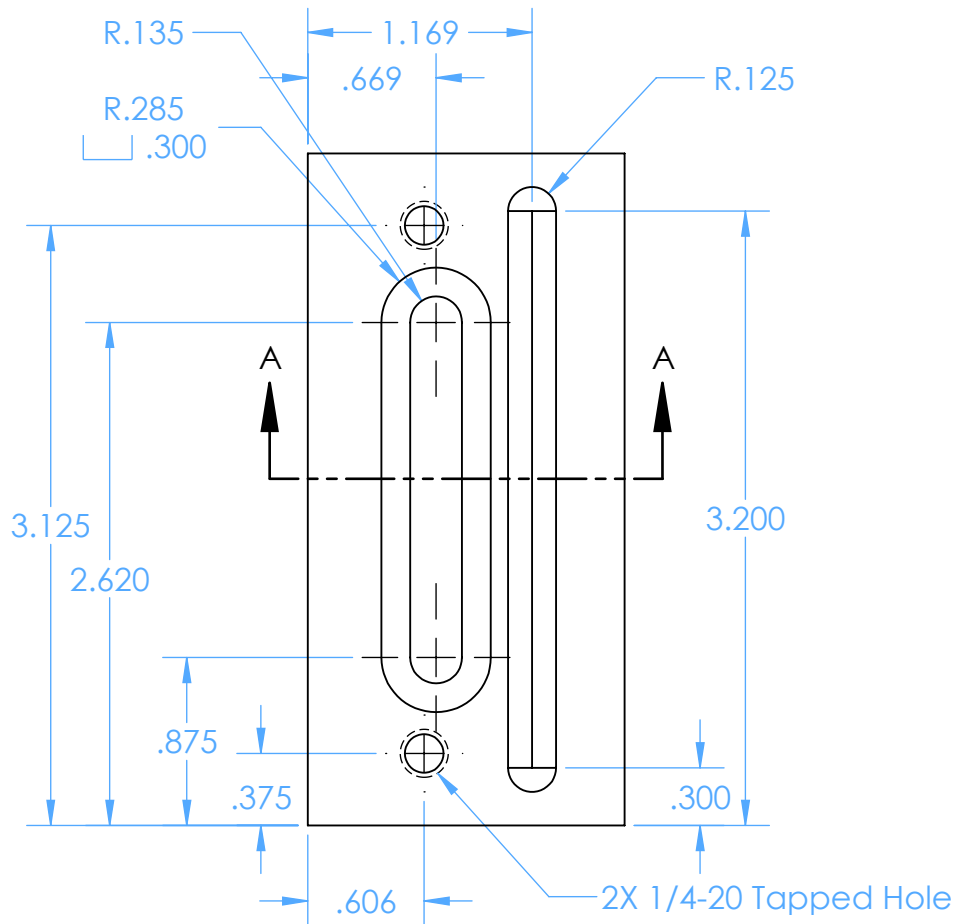
Date: 4/30/2016

Scale: 1:1

Chkd. By: JOHNATHAN SIMEROTH



SECTION A-A



Cal Poly Mechanical Engineering

Tolerance: $\pm .005$

Material: ALU

Title: RIGHT MOUNT

Drwn. By: GRANT POCKLINGTON

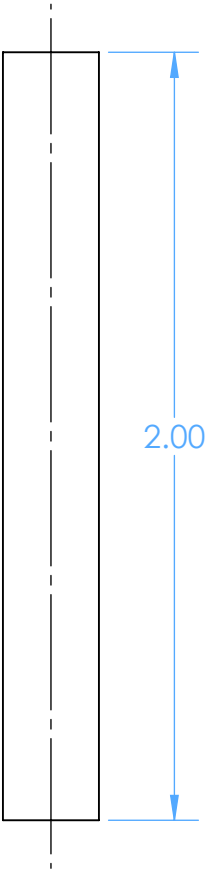
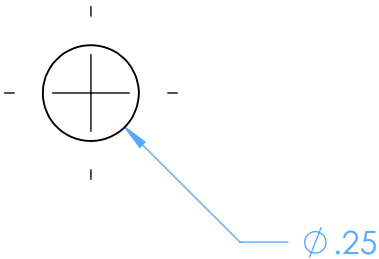
Dwg. #: P010

Nxt Asb: A001

Date: 4/30/2016

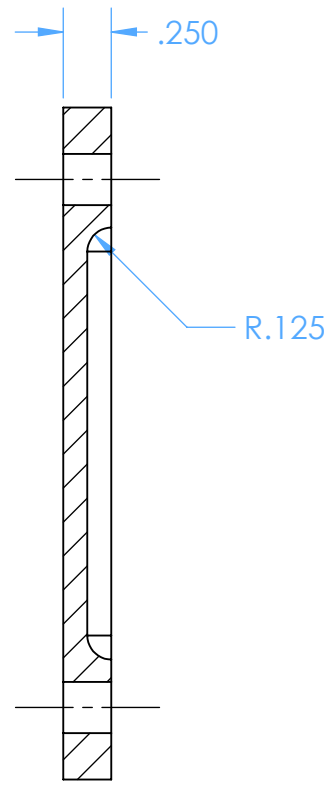
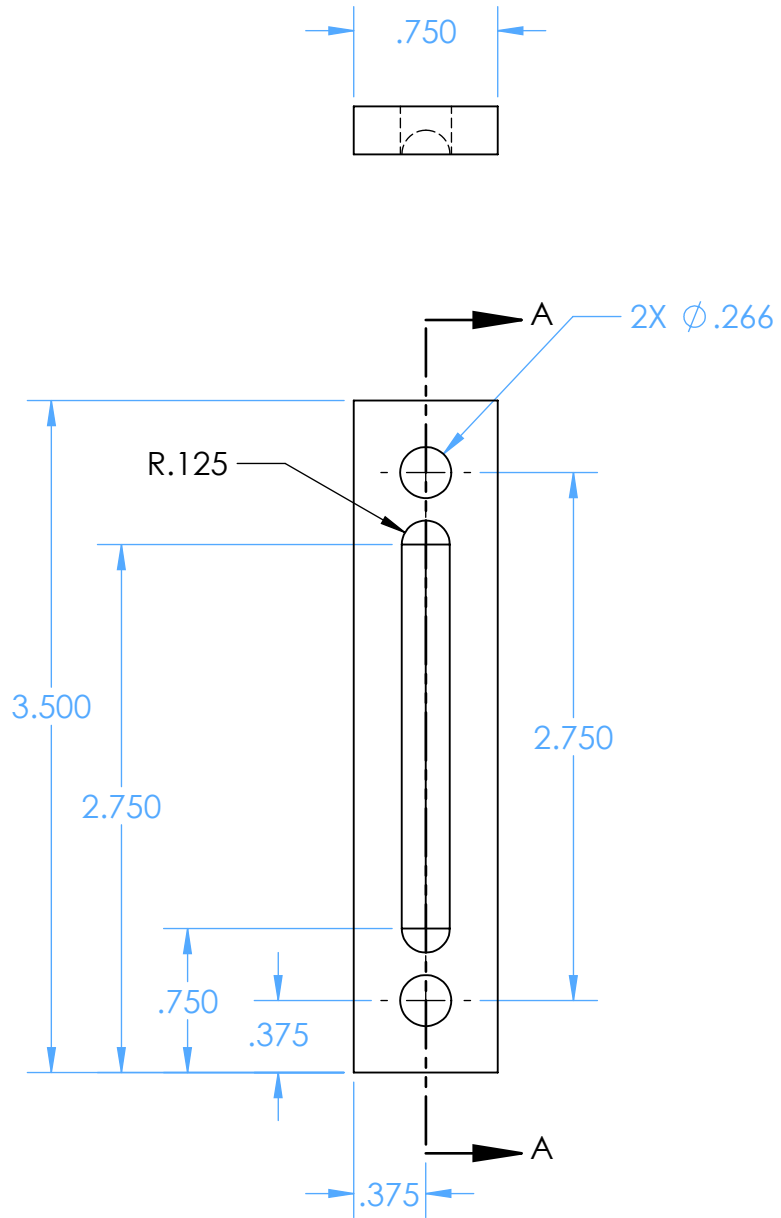
Scale: 1:1

Chkd. By: JOHNATHAN SIMEROTH

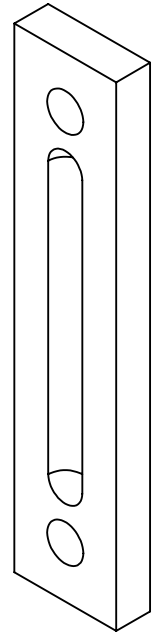


DIAMETER NOMINAL FROM MANUFACTURER

Cal Poly Mechanical Engineering	Tolerance: $\pm .1"$	Material: RUBBER	Title: RUBBER BACKING MATERIAL	Drwn. By: GRANT POCKLINGTON
	Dwg. #: P011	Nxt Asb: A001	Date: 4/30/2016	Scale: 2:1



SECTION A-A



Cal Poly Mechanical Engineering

Tolerance: $\pm .005$

Material: STEEL

Title: OUTER MOUNT

Drwn. By: GRANT POCKLINGTON

Dwg. #: P012

Nxt Asb: A001

Date: 4/30/2016

Scale: 1:1

Chkd. By: JOHNATHAN SIMEROTH

APPENDIX I - SUMMARY OF TESTING INPUTS AND OUTPUTS

Test Variables:			1	2	3	4	5	6	7	8	9	Output
Test Date	Test #	Crank Arm	Pressure Behind Gun	Contact Force	Fixture Used	Clamp Arrangement	Clamp Tightness	Gun Placement (SL=Spindle Lug, PL=Pedal Lug)	Tape	Time Under Vibration	Rubber Hardness	Heat Signature
		(#)	[PSI]	[lbf]	[Describe]	[Describe]	[Describe]	[Relative to lugs]	[Type]	[ms]	[Shore A Durometer]	[Image File Name]
4/5/2016	1	C1	13	23.0	Front Clamps	Both ends clamped	Wrench tightened	.5" right of SL	3M Duct	300	90 Shore A	no file
4/5/2016	2	C1	10	17.7	Front Clamps	Both ends clamped	Wrench tightened	.5" right of SL	3M Duct	300	90 Shore A	no file
4/5/2016	3	C1	6	10.6	Front Clamps	Both ends clamped	Wrench tightened	.5" right of SL	3M Duct	300	90 Shore A	no file
4/5/2016	4	C1	10	17.7	Front Clamps	Both ends clamped	Finger tightened	.5" right of SL	3M Duct	300	90 Shore A	no file
4/5/2016	5	C1	5	8.8	Front Clamps	Both ends clamped	Finger tightened	.5" right of SL	3M Duct	300	90 Shore A	no file
4/5/2016	6	C1	13	23.0	Front Clamps	Only gun side clamped	Finger tightened	.5" right of SL	3M Duct	300	90 Shore A	no file
4/5/2016	7	C1	11	19.4	Front Clamps	Only gun side clamped	Finger tightened	.5" right of SL	3M Duct	300	90 Shore A	no file
4/5/2016	8	C1	11	19.4	Front Clamps	Only gun side clamped	Finger tightened	.5" right of SL	3M Duct	300	90 Shore A	no file
4/5/2016	9	C1	11	19.4	Gun pressure only	N/A	N/A	.5" right of SL	3M Duct	300	90 Shore A	no file
4/5/2016	10	C1	5	8.8	Gun pressure only	N/A	N/A	.5" right of SL	3M Duct	300	90 Shore A	no file
4/5/2016	11	C1	10	17.7	Front Clamps	Only non-gun side clamped	Finger tightened	.5" right of SL	3M Duct	300	90 Shore A	no file
4/5/2016	12	C1	13	23.0	Front Clamps	Only non-gun side clamped	Finger tightened	.5" right of SL	3M Duct	300	90 Shore A	no file
5/17/2016	1	C3	13	23.0	Gun pressure only	N/A	N/A	.5" right of SL	3M Duct	300	90 Shore A	160517 C3 1 13PSI NO CLAMP
5/17/2016	2	F9731	13	23.0	Gun pressure only	N/A	N/A	.5" right of SL	3M Duct	300	90 Shore A	160517 F9731 2 13PSI NO CLAMP
5/17/2016	3	F9738	13	23.0	Gun pressure only	N/A	N/A	.5" right of SL	3M Duct	300	90 Shore A	160517 F9738 3 13PSI NO CLAMP
5/17/2016	4	C3	17	30.0	Gun pressure only	N/A	N/A	.5" right of SL	3M Duct	300	90 Shore A	160517 C3 4 17PSI NO CLAMP
5/17/2016	5	F9731	17	30.0	Gun pressure only	N/A	N/A	.5" right of SL	3M Duct	300	90 Shore A	160517 F9731 5 17PSI NO CLAMP
5/17/2016	6	F9738	17	30.0	Gun pressure only	N/A	N/A	.5" right of SL	3M Duct	300	90 Shore A	160517 F9738 6 17PSI NO CLAMP
5/17/2016	7	C3	15	26.5	Gun pressure only	N/A	N/A	.5" right of SL	3M Duct	300	90 Shore A	160517 C3 7 15PSI NO CLAMP
5/17/2016	8	F9731	15	26.5	Gun pressure only	N/A	N/A	.5" right of SL	3M Duct	300	90 Shore A	160517 F9731 8 15PSI NO CLAMP
5/17/2016	9	F9738	15	26.5	Gun pressure only	N/A	N/A	.5" right of SL	3M Duct	300	90 Shore A	160517 F9738 9 15PSI NO CLAMP
5/17/2016	10	C3	17	30.0	Gun pressure only	N/A	N/A	.5" right of PL	3M Duct	300	90 Shore A	160517 C3 10 17PSI PEDAL
5/17/2016	11	F9731	17	30.0	Gun pressure only	N/A	N/A	.5" right of PL	3M Duct	300	90 Shore A	160517 F9731 11 17PSI PEDAL
5/17/2016	12	F9738	17	30.0	Gun pressure only	N/A	N/A	.5" right of PL	3M Duct	300	90 Shore A	160517 F9738 12 17PSI PEDAL
5/17/2016	13	C3	17	30.0	Gun pressure only	N/A	N/A	On solid side of SL	3M Duct	300	90 Shore A	160517 C3 13 17PSI spindle back side
5/17/2016	14	F9731	17	30.0	Gun pressure only	N/A	N/A	On solid side of SL	3M Duct	300	90 Shore A	160517 F9731 14 17PSI spindle back side
5/17/2016	15	C3	17	30.0	Gun pressure only	N/A	N/A	Back side .5" from PL	3M Duct	300	90 Shore A	160517 C3 15 17PSI pedal back side
5/17/2016	16	F9731	17	30.0	Gun pressure only	N/A	N/A	Back side .5" from PL	3M Duct	300	90 Shore A	160517 F9731 16 17PSI PEDAL back side
5/17/2016	17	F9738	17	30.0	Gun pressure only	N/A	N/A	Back side .5" from PL	3M Duct	300	90 Shore A	160517 F9738 17 17PSI PEDAL back side
5/17/2016	18	C3	17	30.0	Gun pressure only	N/A	N/A	Back Side between center and SL	3M Duct	300	90 Shore A	160517 C3 18 17PSI left mid spindle back side
5/17/2016	19	F9731	17	30.0	Gun pressure only	N/A	N/A	Back Side between center and SL	3M Duct	300	90 Shore A	160517 F9731 19 17PSI left mid spindle back side
5/17/2016	20	F9738	17	30.0	Gun pressure only	N/A	N/A	Back Side between center and SL	3M Duct	300	90 Shore A	160517 F9738 20 17PSI left mid spindle back side
5/24/2016	1	C3	15	26.5	Spindle Mount	N/A	N/A	Pedal Spindle Plug	3M Duct	300	N/A	160524 3 1 15psi spindle
5/24/2016	2	F9731	15	26.5	Spindle Mount	N/A	N/A	Pedal Spindle Plug	3M Duct	300	N/A	160524 F9731 2 15psi spindle
5/24/2016	3	F9731	17	30.0	Spindle Mount	N/A	N/A	Pedal Spindle Plug	3M Duct	300	N/A	160524 F9731 3 17psi spindle
5/24/2016	4	F9731	17	30.0	Spindle Mount	N/A	N/A	Pedal Spindle Plug	3M Duct	300	N/A	160524 F9731 4 17psi spindle teflon
5/24/2016	5	F9738	17	30.0	Spindle Mount	N/A	N/A	Pedal Spindle Plug	3M Duct	300	N/A	160524 F9738 5 17psi spindle
5/24/2016	6	F9738	6	10.6	Spindle Mount	N/A	N/A	Pedal Spindle Plug	3M Duct	300	N/A	160524 F9738 6 6psi spindle
5/24/2016	7	F9738	10	17.7	Spindle Mount	N/A	N/A	Pedal Spindle Plug	3M Duct	300	N/A	160524 F9738 7 10psi spindle
5/24/2016	8	F9731	17	30.0	Spindle Mount	N/A	N/A	Pedal Spindle Plug	3M Duct	300	N/A	160524 F9731 8 17psi spindle
5/24/2016	9	C3	17	30.0	Spindle Mount	N/A	N/A	Pedal Spindle Plug	3M Duct	300	N/A	160524 3 9 17psi spindle
5/24/2016	10	C3	17	30.0	Spindle Mount	N/A	N/A	.5" right of PL	3M Duct	300	N/A	160524 3 10 17psi spindle near pedal
5/24/2016	11	F9738	17	30.0	Spindle Mount	N/A	N/A	.5" right of PL	3M Duct	300	N/A	160524 F9738 11 17psi spindle near pedal
5/24/2016	12	F9731	17	30.0	Spindle Mount	N/A	N/A	.5" right of PL	3M Duct	300	N/A	160524 F9731 12 17psi spindle near pedal
5/24/2016	13	F9731	17	30.0	Spindle Mount	N/A	N/A	.5" right of SL	3M Duct	300	N/A	160524 F9731 13 17psi spindle near spindle
5/24/2016	14	C3	17	30.0	Spindle Mount	N/A	N/A	.5" right of SL	3M Duct	300	N/A	160524 3 14 17psi spindle near spindle
5/24/2016	15	C3	17	30.0	Spindle Mount	N/A	N/A	.5" right of SL	3M Duct	300	N/A	160524 3 15 17psi spindle near spindle2
5/24/2016	16	F9738	17	30.0	Spindle Mount	N/A	N/A	.5" right of SL	3M Duct	300	N/A	160524 F9738 16 17psi spindle near spindle2
5/24/2016	17	F9731	17	30.0	Spindle Mount	N/A	N/A	.5" right of SL	3M Duct	300	N/A	160524 F9731 17 17psi spindle near spindle2
5/24/2016	18	C4	17	30.0	Spindle Mount	N/A	N/A	.5" right of PL	3M Duct 8x	300	N/A	---
5/24/2016	19	C4	17	30.0	Spindle Mount	N/A	N/A	.5" right of PL	3M Duct 20x	300	N/A	---
5/24/2016	20	F9731	17	30.0	Spindle Mount	N/A	N/A	.5" right of PL	3M Duct 20x	300	N/A	7

References

- [1] Several types of a composite laminate after impact testing. Digital image. What-when-how. N.p., n.d. Web. 3 May 2016.
<<http://what-when-how.com/experimental-and-applied-mechanics/drop-weight-impact-studies-of-glare-5-fiber-metal-laminates-experimental-and-applied-mechanics-part-1/>>.
- [2] "Crushing Victory on SRAM 1x™." SRAM. N.p., n.d. Web. 03 May 2016.
<<https://www.sram.com/stories/crushing-victory-sram-1x>>.
- [3] The Visual Differences Between Unidirectional CFRP, and Two Different Fiber Counts For Woven CFRP. Digital image. *Jack Kane Custom Racing Bicycles*. Jack Kane Custom Racing Bicycles, n.d. Web. 21 Feb. 2016.
- [4] Deville, Sylvain, Eduardo Said, and Antoni P. Tomsia. Figure 4: SEM Micrographs of the Porous Structure: (a) Isotropic vs. (b) Anisotropic Microstructure. Digital image. Research Gate. Materials Sciences Division, Lawrence Berkeley National Laboratory, 08 Dec. 2015. Web. 3 May 2016. <https://www.researchgate.net/publication/223164088_Ice-Templated_Porous_Alumina_Structures>.
- [5] Campbell, F. C. "Introduction to Composite Materials." *Structural Composite Materials*. Materials Park: ASM International, 2010. 1-31. Print.
- [6] Sojasi, Saeed, Fariba Khodayar, Fernando Lopez, Clemente Ibarra-Castando, Xavier Maldague, Vladimir P. Vavilov, and Arseny O. Chulkov. *Infrared Testing of CFRP Components: Comparisons of Approaches Using the Tanimoto Criterion*. Publication. Edmonton: n.p., 2015. Print.
- [7] Renshaw, Jeremy, John C. Chen, Stephen D. Holland, and R. Bruce Thompson. *The Sources of Heat Generation in Vibrothermography*. N.p.: n.p., n.d. Print.
- [8] Kapadia, Ajay, and TWI Ltd. *Non Destructive Testing of Composite Materials*. N.p.: National Composites Network, n.d. Print.
- [9] UNNÞÓRSSON, RÚNAR, M. T. Jonsson, and T. P. Runarsson. *NDT Methods for Evaluating Carbon Fiber Composites*. Tech. Reykjavik: U of Iceland, 2004. Web. 01 Feb. 2016.
- [10] Szwedlo, M., L. Pieczonka, and T. Uhl. *Application of Vibrothermography in Nondestructive Testing of Structures*. Rep. Krakow: n.p., n.d. Print.
- [11] Abbaszadeh, Ben, and Elisha Muir. *Lock-In Thermography*. Rep. N.p.: n.p., n.d. Presentation.
- [12] Chen, John C., Joseph D. Mello, and Luz Elena Gomez. Designed Defects in Laminate Composites. Cal Poly Corporation, San Luis Obispo, CA (US), assignee. Patent US 8,865,296 B2. 21 Oct. 2014. Print.

[13] Pieczonka, Lukasz. *The Influence of Excitation Frequency on the Effectiveness of Vibrothermographic Testing*. Publication. Vol. 15. Krakow: n.p., 2014. Print. Diagnostyka.